

1 **Title:Ice records provide new insights into climatic vulnerability of**  
2 **Central Asian forest and steppe communities**  
3

4 Short title: Vulnerability of forest-steppe communities

5 Authors: Sandra O. Brugger<sup>a,b</sup>, Erika Gobet<sup>a,b</sup>, Michael Sigl<sup>b,c</sup>, Dimitri Osmont<sup>b,c,d</sup>, Tatyana  
6 Papina<sup>e</sup>, Natalia Rudaya<sup>f,g</sup>, Margit Schwikowski<sup>b,c,d</sup>, Willy Tinner<sup>a,b</sup>

7 <sup>a</sup>Institute of Plant Sciences, University of Bern, Switzerland

8 <sup>b</sup>Oeschger Center for Climate Change Research, University of Bern, Switzerland

9 <sup>c</sup>Paul Scherrer Institute, Villigen, Switzerland

10 <sup>d</sup>Department for Chemistry and Biochemistry, University of Bern, Switzerland

11 <sup>e</sup>Institute for Water and Environmental Problems, SB RAS, Barnaul, Russia

12 <sup>f</sup>Institute of Archaeology and Ethnography, SB RAS, Novosibirsk, Russia

13 <sup>g</sup>University of Potsdam, Germany

14  
15 Contact corresponding author: Address: Institute of Plant Sciences, Altenbergrain 21, CH-3013  
16 Bern, email: sandra.bruegger@ips.unibe.ch, phone: +41 79 288 73 52

17 Keywords: Boreal forest diebacks, Climatic tipping points, Diversity, Ice core, Moisture  
18 change, Pollen, Microscopic charcoal, SCP

19  
20 Declarations of interest: none

21 **ABSTRACT**

22 Forest and steppe communities in the Altai region of Central Asia are threatened by changing  
23 climate and anthropogenic pressure. Specifically, increasing drought and grazing pressure may  
24 cause collapses of moisture-demanding plant communities, particularly forests. Knowledge  
25 about past vegetation and fire responses to climate and land use changes may help anticipating  
26 future ecosystem risks, given that it has the potential to disclose mechanisms and processes that  
27 govern ecosystem vulnerability. We present a unique paleoecological record from the high-  
28 alpine Tsambagarav glacier in the Mongolian Altai that provides novel large-scale information  
29 on vegetation, fire and pollution with an exceptional temporal resolution. Our palynological  
30 record identifies several late-Holocene boreal forest expansions, contractions and subsequent  
31 recoveries. Maximum forest expansions occurred at 3000–2800 BC, 2400–2100 BC, and 1900–  
32 1800 BC. After 1800 BC mixed boreal forest communities irrecoverably declined. Fires reached  
33 a maximum at 1600 BC, 200 years after the final forest collapse. Our multiproxy data suggest  
34 that burning peaked in response to dead biomass accumulation resulting from forest diebacks.  
35 Vegetation and fire regimes partly decoupled from climate after 1700 AD, when atmospheric  
36 industrial pollution began, and land use intensified. We conclude that moisture availability was  
37 more important than temperature for past vegetation dynamics, in particular for forest loss and  
38 steppe expansion. The past Mongolian Altai evidence implies that in the future forests of the  
39 Russian Altai may collapse in response to reduced moisture availability.

## 40 INTRODUCTION

41 Forest disruption has substantially increased globally in recent years (McDowell & Allen,  
42 2015). The vast boreal forests and forest steppes in and around the Altai region in Central Asia  
43 provide an important terrestrial carbon storage but respond highly sensitive to recent global  
44 change (Sato et al., 2007; Liu et al., 2013; Chenlemuge et al., 2013; Tian et al., 2013; 2014;  
45 Hijjoka et al., 2014; Dulamsuren et al., 2016; Khansaritoreh et al., 2017; Zaoh et al., 2018). In  
46 the past decades, the Altai region experienced rising temperatures combined with increasing  
47 extreme events such as prolonged heatwaves, drought periods and short-term heavy rainfall  
48 events (Lkhagvadorj et al., 2013). As boreal forest growth is not only limited by temperature  
49 but also by moisture availability, the forests progressively suffer from water constraints  
50 (Dulamsuren et al., 2010; 2014). The establishment, persistence and decline of these boreal  
51 forests depend on soil moisture availability which is not only constrained by precipitation, but  
52 also by the local soil development and its water-holding capacity (Henne et al., 2011) that is  
53 extremely low for the predominant soil types in the region.

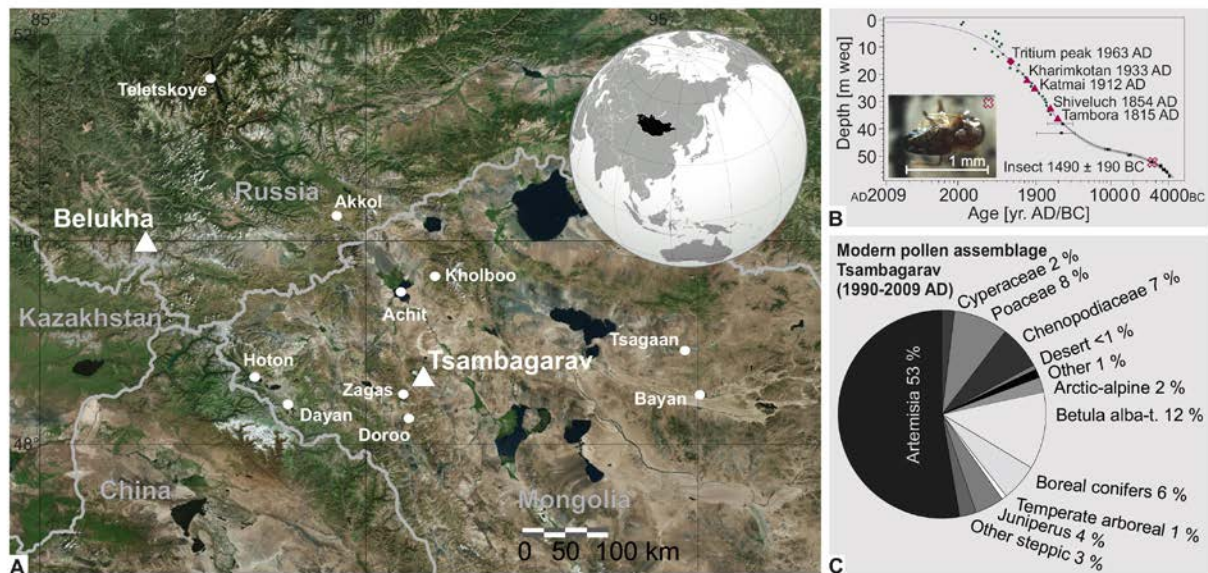
54 The central position of the Altai Mountains between the vast Siberian Taiga forests in the  
55 north and the Gobi desert in the south results in a steep climatic and vegetation gradient with  
56 fragmented and diverse habitats including many rare and endemic species (Rudaya et al., 2008).  
57 Their natural resources such as forests, productive grasslands, and fresh water sources have  
58 attracted Central Asian nomadic groups since centuries (Rudaya et al., 2008). In recent years,  
59 these ecotonal mountain steppe ecosystems experienced rapid degradation through over-  
60 grazing, systematic logging, dead wood collecting and human-set fires (Tsogtbaatar, 2004;  
61 Dulamsuren et al., 2014). Anthropogenic pressure combined with growing moisture deficiency  
62 may cause irreversible forest vegetation loss, reduce steppe pasture productivity and thus alter  
63 species composition and diversity (Lkhagvadorj et al., 2013).

64 Knowledge about past vegetation dynamics in the Mongolian Altai contributes to a better  
65 understanding of future ecosystem responses to climate change and human land use, and may  
66 assist forest, grassland and fire management strategies by providing baselines of past ecosystem

67 variability in response to strong environmental change. However, paleo records that provide  
68 information about Holocene vegetation and fire history are scarce, lack temporal resolution  
69 and/or chronological precision (Tarasov et al., 2000; Gunin et al., 2009; Rudaya et al., 2009;  
70 Umbanhowar et al., 2009; Unkelbach et al., 2018). Such limitations impede a thorough  
71 assessment of ecosystem resilience and vulnerability. The snow-capped Tsambagarav  
72 Mountain provides a regional to supra-regional ice archive of ecosystem change, which is well  
73 suited to reconstruct ecosystem dynamics with high temporal resolution and precision (Herren  
74 et al., 2009). Here we address persisting knowledge gaps with the following aims: (1) for the  
75 first time, we use microscopic charcoal to reconstruct the fire dynamics in the Mongolian Altai;  
76 (2) pollen, spores and spheroidal carbonaceous particles are used to investigate the long-term  
77 linkages between the fire regime, vegetation, land use, and pollution; (3) we use the  
78 palynological information including charcoal to assess ecosystem response variability to  
79 climate change, and (4) evidence from other studies is used to underscore the spatio-temporal  
80 relevance of our outcomes and to derive implications for ecosystem responses under global-  
81 change conditions.

## 82 **STUDY SITE**

83 The Altai Mountains stretch over ca. 1200 km, crossing the borders of Russia, Mongolia,  
84 Kazakhstan, and China. With 4500 m a.s.l. maximum elevation (Mount Belukha in Russia, Fig.  
85 1A) the Altai Mountains build a continental climate barrier for air masses from northwest,  
86 resulting in a strong northwest ( $800 \text{ mm year}^{-1}$ ) to southeast ( $<200 \text{ mm year}^{-1}$ ) precipitation  
87 gradient (Klinge et al., 2003) given that the moisture source in the region are the Westerlies.  
88 The extreme continental climate is dominated by the Siberian High with cold dry winters and  
89 precipitation prevailing in June to August (Klinge et al., 2003). The investigated ice archive on  
90 Tsambagarav Mountain is located in the Mongolian Bayan-Ölgii province (Fig. 1A), a region  
91 with very dry climatic conditions (annual precipitation ca. 200 mm at 1700 m a.s.l.).



92

93 **Figure 1 Study area, chronology and modern pollen deposition at Tsambagarav glacier.** Panel A: Map of the Altai region  
 94 with glacier records (triangle) and selected records of fire and vegetation reconstructions (white dots), map modified (source  
 95 of satellite images: U.S. Geological Survey). Panel B: Chronology of Tsambagarav record based on a glacier flow model (blue  
 96 dashed line), annual layer counting (2009–1815 AD), maximum tritium peak (red diamond), volcanic layers (red triangles) and  
 97 <sup>210</sup>Pb activity (green circles). From 1815 AD modeled ages as exponential equation (black dashed line) with upper and lower  
 98 limit of the equation (gray shaded) based on <sup>14</sup>C- dating of water-insoluble organic carbon of atmospheric origin (black squares  
 99 with uncertainty bars). Insert: <sup>14</sup>C-date of an insect remain (red cross and photo, Uglietti et al., 2016). Figure adapted from  
 100 Herren et al. (2013). Panel C: Modern pollen assemblage in Tsambagarav glacier ice (average over 20 years as percentages of  
 101 the terrestrial pollen sum).

102 Geologically, the Mongolian Altai consists of siliceous bedrock, including schists and  
 103 granites with Leptosols as prevailing soil type that are susceptible to erosion and desiccation  
 104 (Dulamsuren et al., 2014). The modern vegetation around Tsambagarav reflects the cold semi-  
 105 arid continental climate characterized by huge differences in maximum and minimum daily and  
 106 yearly temperatures (July average +22.7 °C, January average -22.6 °C at Ölgii weather station;  
 107 NOAA, 2013). Gradients such as altitude and exposure lead to pronounced local differences in  
 108 growth season length, heat sum, precipitation, and soil formation, which together strongly affect  
 109 species distribution and productivity (Rudaya et al., 2009).

110 Wide areas at high elevations surrounding Tsambagarav are occupied by cryo-xerophyllic  
 111 mountain steppe communities mainly composed of *Festuca sulcata* sp., *Poa botryoides*, *Carex*  
 112 *pediformis*, but also *Artemisia frigida* and *A. tanacetifolia* (Walter, 1974). Alpine tundra  
 113 communities with *Betula nana* ssp. *rotundifolia* (synonyms *Betula nana* subsp. *rotundifolia*  
 114 (Spach) Malyshev, *Betula glandulosa* Michaux subsp. *rotundifolia* (Spach) Regel, and *Betula*  
 115 *rotundifolia* Spach, see TPL, 2018; Gunin et al., 2009), *Salix glauca*, *Kobresia*, and *Potentilla*  
 116 *sericea* become more abundant with increasing altitude and may penetrate up to 3000 m a.s.l.

117 (Walter, 1974). High alpine *Kobresia* meadows with *Poa altaica*, *P. sibirica*, *Festuca*, *Carex*  
118 and *Thalictrum alpinum* are increasingly fragmented above 3200 m a.s.l. *Sedum algidum* is  
119 found up to the nival zone close to the eternal snow margin (Walter, 1974), which is at  
120 Tsambagarav between 3000 to 3800 m a.s.l. depending on the exposure (Herren et al., 2013).  
121 Below 1800–2000 m a.s.l. the mountain steppes are gradually replaced by dry *Stipa-Artemisia*  
122 steppe communities with *Stipa glareosa*, *S. gobica*, *Allium*, *Tanacetum*, *Artemisia* species, and  
123 *Caragana* (Walter, 1974; Gunin et al., 2009). *Anabasis brevifolia* (Chenopodiaceae) is the most  
124 common halophilous taxon in the region. Desert-steppe communities composed of *Stipa* sp. and  
125 *Salsola* dominate in dry isolated valleys and southeast of Tsambagarav in the large mountain  
126 depression “basin of the large lakes”, where precipitation is further reduced to <200 mm year<sup>-1</sup>  
127 (Gunin et al., 2009). Wet herbaceous communities and small woody stands with *Betula*  
128 *pendula*, *Populus tremula*, *Salix*, and *Alnus glutinosa* grow along streams (Walter, 1974; Gunin  
129 et al., 2009; Stritch et al., 2014). The closest of these parklands with dozens of km<sup>2</sup> sizes occur  
130 ca. 50 km northwest of Tsambagarav.

131 The mid-elevation forest belt in the Mongolian Altai is restricted to north facing slopes in  
132 the western (Hoton Nur area, Fig. 1A) and northwestern part of the Mongolian Altai between  
133 1900–2100 m a.s.l., while on south facing slopes, mountain steppe communities directly pass  
134 over to alpine plant communities. The narrow and discontinuous forest belts are composed of  
135 *Pinus sibirica*, *Larix sibirica*, *Betula pendula*. *Picea obovata* co-occurs where soil moisture is  
136 sufficient (Walter, 1974; Gunin et al., 2009). In these forest stands at ca. 100 km distance from  
137 Tsambagarav, the upper limit of tree growth is controlled by summer temperature and the lower  
138 limit by moisture availability and anthropogenic pressure such as logging activities (Klinge et  
139 al., 2003; Lkhagvadorj et al., 2013; Tsogtbaatar, 2013). Floristically, the Mongolian forest  
140 relicts belong to the forests in the Russian Altai (Walter, 1974) which consist of *Pinus sibirica*,  
141 *Abies sibirica*, *Larix sibirica* and *Betula pendula* that form a dense boreal forest belt between  
142 ca. 1000 and 2000 m a.s.l. in the region north of the Belukha glacier (see Fig. 1A; Walter, 1974;  
143 *Eichler et al., 2011*). Below 1000 m a.s.l the Russian Altai is characterized by lowland feather-

144 grass steppes (*Stipa*, other Poaceae, *Artemisia*, and Chenopodiaceae; Walter, 1974). Modern  
145 *Pinus sylvestris* and *Abies sibirica* distribution is restricted to the Russian and Kazakh Altai, ca.  
146 150–200 km north of Tsambagarav (Gunin et al., 2009).

## 147 MATERIAL AND METHODS

### 148 Ice material and microfossil analysis

149 We analyzed samples from an existing ice core from Tsambagarav Mountain. The core was  
150 drilled on the eastern summit (48° 39.338' N, 90° 50.826' E; Fig. 1A) in July 2009 at an altitude  
151 of 4130 m a.s.l. (Herren et al., 2013). The drilling reached bedrock with a total ice core length  
152 of 72 m and a diameter of 8.2 cm. Core segments of ca. 70 cm were transported frozen to the  
153 Paul Scherrer Institute (PSI) in Switzerland.

154 202 continuous samples spanning the time 3500 BC to 2009 AD (55.6–0 m weq = water  
155 equivalent, corrected for varying density) from the outer part of the ice core were taken for  
156 palynological analysis. The sampling resolution was 40–90 years (3500 BC–1200 AD), 20–30  
157 years (1200–1650 AD), 10 years (1650–1700 AD), five years (1700–1985 AD), and one year  
158 (1985–2009 AD, merged to five years after analysis) using the chronology of Herren et al.  
159 (2013). An additional <sup>14</sup>C-date from an insect remain found during palynological sampling  
160 confirmed the accuracy of the existing depth-age model (Fig. 1B; Uglietti et al., 2016). Each  
161 sample contained 200–400 g ice, except one sample with 45 g at 52.2 m weq. The microfossil  
162 extraction followed a protocol for ice sample preparation (Brugger et al., 2018). One  
163 *Lycopodium* tablet was added to each sample before lab treatment to estimate microfossil  
164 concentrations (Stockmarr, 1971). Due to strong thinning in the deeper part of the glacier caused  
165 by lateral ice flow, annual layers could not be identified before 1825 AD, preventing influx  
166 calculations with a reasonable time resolution.

167 We use pollen and spores to infer vegetation history and the coprophilous fungal spore  
168 *Sporormiella* as a proxy for herbivore grazing activity. A pollen sum of 500 was reached except  
169 in the samples of section 54–53 m weq (2600–2000 BC), where due to small pollen

170 concentrations we reached 100 grains, which is above the minimum for reliable percentage  
171 calculations and environmental reconstructions (50 items; Heiri and Lotter, 2001). Pollen and  
172 spore identification under a light microscope at 400 x magnification followed palynological  
173 keys (Huang, 1972; Moore et al., 1991; Beug, 2004) and the reference collection in Bern,  
174 Switzerland. Shrub type (referred to as *Betula nana*-type) and tree type *Betula* (*Betula alba*-  
175 type) separation is based on the pore depth and the grain diameter to pore depth ratio (D/P)  
176 following Clegg et al. (2015). The palynological *Betula* distinction covers *B. pubescens*, *B.*  
177 *pendula* (both *B. alba*-type), *B. glandulosa* and *B. nana* (both *B. nana*-type) as well as other  
178 North American and Eurasian birch species (Birks, 1968; Clegg et al., 2015). Cerealia-type was  
179 classified according to Beug (2004). Although *Artemisia* comprises herb and shrub species, we  
180 include all *Artemisia* pollen in the herb pollen sum following Gunin et al. (2009) since pollen  
181 taxonomy allows no further discrimination. Pollen and spore data are presented as percentages  
182 of the terrestrial pollen sum.

183 Microscopic charcoal >10  $\mu\text{m}$  is used as a proxy for fire activity (e.g. MacDonald et al.,  
184 1991; Tinner et al., 1998; Conedera et al., 2009; Adolf et al., 2017). We counted a minimum  
185 sum of 200 items (charcoal fragments and *Lycopodium* grains, Finsinger & Tinner, 2005;  
186 Tinner & Hu, 2003). If needed (low charcoal concentrations), we continued until a minimum  
187 of 20 charcoal fragments was reached. Subsequently, the > 90th percentile (= 10 % upper  
188 charcoal concentration values over the entire record) was identified to infer regional fire activity  
189 peaks. SCP (= spheroidal carbonaceous particles) with a diameter >10  $\mu\text{m}$  and clear features  
190 (Rose, 2015) were counted along pollen and spores to reconstruct industrial air pollution. All  
191 microfossil concentrations were standardized to one liter.

192 Annual layer thickness is highest in the uppermost part of the ice core, resulting in an  
193 exponential depth-age relationship (Fig. 1B). Thus, the temporal sampling resolution in the  
194 younger part is much higher compared to the older part of the ice core where the ice had thinned  
195 substantially (i.e. one to several hundred years per m weq with increasing core depth). These  
196 archive characteristics result in varying detection limits for rare microfossil types along the



197 record for comparable time periods. We kept the original lab sampling resolution for the  
198 interpretation of the palynological record (Figs 2–4) while we amalgamated samples of the  
199 overview pollen and charcoal records to reach 40 to 50 years resolution in the younger part  
200 (period 1100–2009 AD, Fig. 5). This resulted in comparable time steps along the sequence.

## 201 **Numerical analysis**

202 Optimal sum-of-squares partitioning was applied for zonation of the pollen data (Birks &  
203 Gordon, 1985). Subsequently, statistically significant local pollen assemblage zones (LPAZ)  
204 were inferred with the broken stick approach (Bennett, 1996). Only LPAZ with more than two  
205 samples were accepted to account for single microfossil deposition events reaching the exposed  
206 high-alpine glacier site. We applied ordination methods to statistically summarize the pollen  
207 signal and to search for correlations with supplementary variables and similarities with external  
208 data. The short gradient length of the first axis (= 1.35) of a detrended correspondence analysis  
209 (DCA, detrended by segments) justifies using linear ordination methods (ter Braak & Prentice,  
210 1988). Therefore, we applied principal component analysis (PCA) based on a correlation  
211 matrix. Charcoal concentrations, fern spore and *Sporormiella* percentages of the Tsambagarav  
212 data were included as supplementary variables (Fig. 4) and pollen percentages from Belukha  
213 glacier (Eichler et al., 2011) were included as external samples (not influencing the ordination  
214 dataset) to search for spatio-temporal similarities between the two sites. We amalgamated  
215 *Betula* (includes *Betula nana*-type and *Betula alba*-type) and Chenopodiaceae (*Salsola* and  
216 remaining Chenopodiaceae) to homogenize the taxonomic resolution between the Tsambagarav  
217 and Belukha data.

218 To our knowledge palynologically-based diversity measures (e.g. palynological richness,  
219 evenness) are not available yet from the Altai region. To fill this gap we estimated palynological  
220 richness (PRI) with rarefaction analysis as a proxy for species richness and the probability of  
221 interspecific encounter (PIE) as a proxy for evenness (Birks & Line, 1992; Hurlbert, 1971). The  
222 minimum pollen sum for rarefaction analysis was 105 pollen grains. To account for evenness

223 distortions of palynological richness we calculated PIE-detrended palynological richness (DE-  
224 PRI; Colombaroli & Tinner, 2013).

## 225 **RESULTS AND INTERPRETATION**

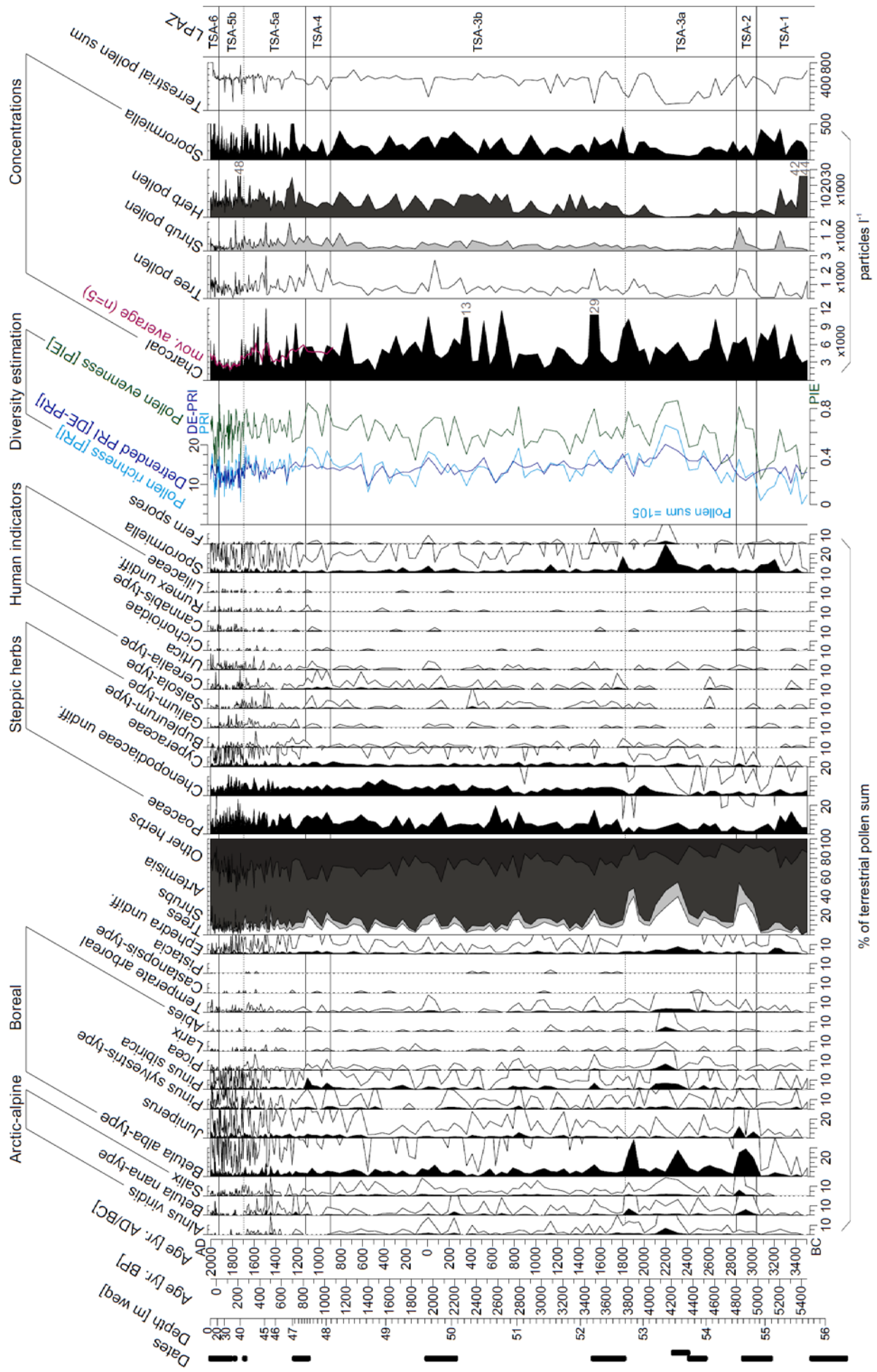
### 226 **Modern pollen composition reflects vegetation and pollen catchment**

227 The modern pollen concentration in the Tsambagarav record is ca. 6000 grains l<sup>-1</sup> which  
228 corresponds to a total influx of 450 grains cm<sup>-2</sup> year<sup>-1</sup>. This is very low compared to sedimentary  
229 archives. The largest amount derives from the steppic taxa *Artemisia* (53 %), Poaceae (8 %)  
230 and Chenopodiaceae (7 %), with arboreal pollen (AP) of *Betula alba*-type (12 %), *Juniperus* (4  
231 %), and conifers such as *Pinus sibirica* (6 %; Fig. 1C). With 25 % AP and 75 % non-arboreal  
232 pollen (NAP) the pollen signal reflects the patchy modern regional vegetation dominated by  
233 dry herbaceous steppes with scattered boreal trees. The presence of conifer and *Betula* pollen  
234 indicates regional sources, as the closest parklands with *Betula pendula* (*Betula alba*-type  
235 pollen) occur at ca. 50 km northwestwards and forested areas around 100 km westwards in the  
236 Hoton Nur region (Fig. 1A). Single grains of warm-loving taxa (e.g. *Castanopsis*-type and  
237 *Pistacia*; Fig. 2) along the record indicate pollen transport by southern air masses over more  
238 than 1000 km, where *Pistacia* has its northern distribution limit today (Golan-Goldhirsh, 2009).  
239 Westerlies are the main moisture source for the Altai region. On the basis of the modern  
240 atmospheric pattern (Herren et al., 2013) we assume northwest as the predominant wind  
241 direction for our site during the mid and late Holocene. The historical pollen assemblages at  
242 Tsambagarav are clearly distinct from those from Belukha glacier in the Russian Altai ca. 320  
243 km northwest (Fig. 1 A; Eichler et al., 2011). This finding suggests little overlap of the two  
244 glacier pollen catchments. Based on the pollen composition in the top sample of Tsambagarav  
245 and its comparison with vegetation composition in the study area (e.g. Walter 1974; Gunin et  
246 al., 2009) we assume that the Tsambagarav pollen signal derives from a catchment of ca. 60–  
247 200 km around the site, most likely with a strong northwest bias and with only occasional pollen  
248 grains deriving from longer distances.

249 **Vegetation history**

250 Six statistically significant local pollen assemblage zones (LPAZ) were identified along the  
251 palynological record (Figs 2–3). We additionally divided TSA-3 and TSA-5 in two non-  
252 significant subzones a and b. Results are presented as pollen percentages and pollen  
253 concentrations (around 10'000 grains l<sup>-1</sup> except the period 2900–1800 BC (zone TSA-3a) with  
254 low concentrations <2000 grains l<sup>-1</sup>).

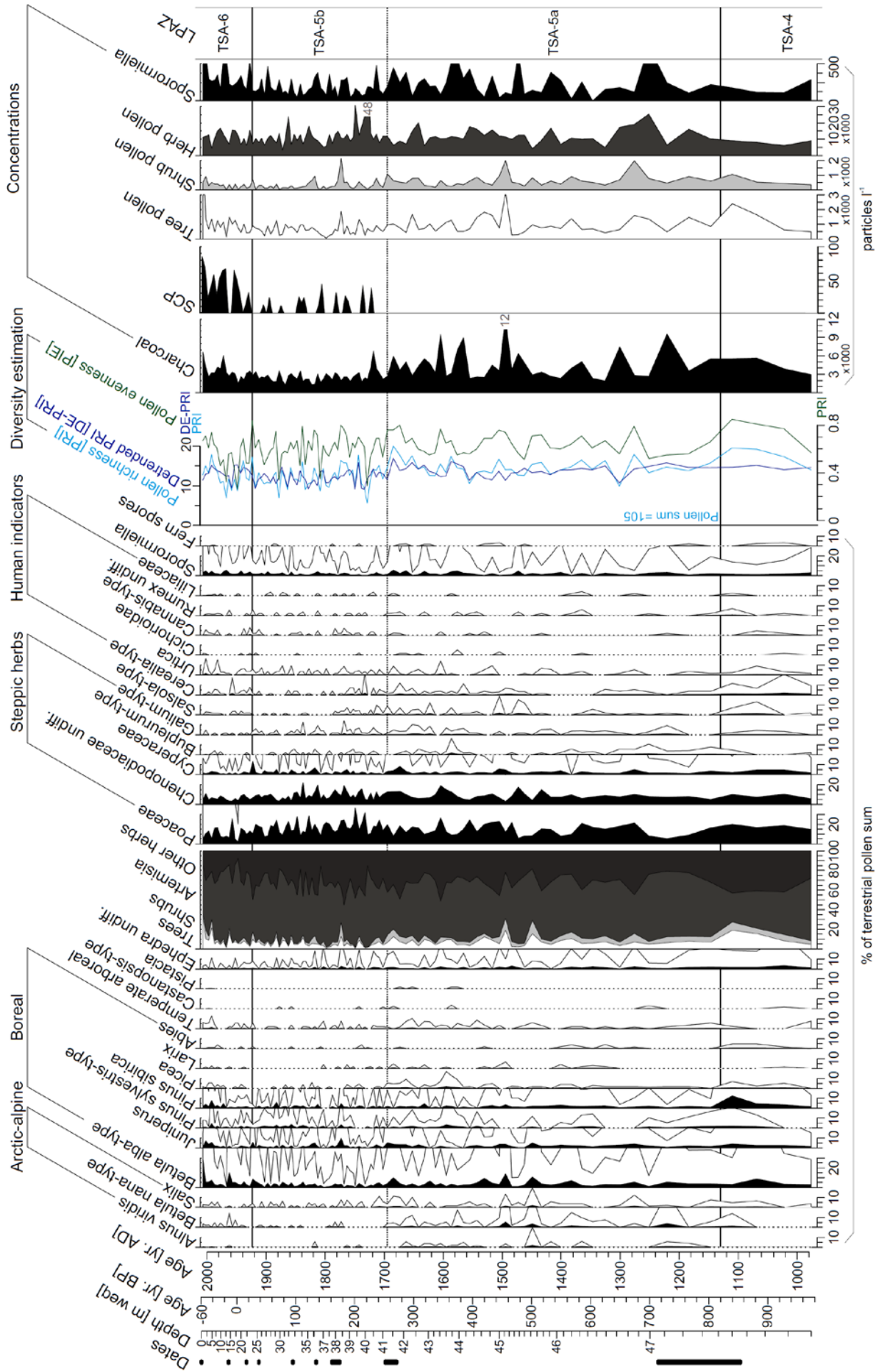
255 Pollen data in zone TSA-1 (3500–3100 BC) indicates that the vegetation was dominated by  
256 herbaceous steppe communities, mainly composed of *Artemisia* (80 %) with Poaceae,  
257 Chenopodiaceae and other taxa growing in dry *Stipa-Artemisia* steppe communities (e.g.  
258 Cyperaceae, *Bupleurum*-type, *Galium*-type; Fig. 2). The pollen record indicates that *Salsola*, a  
259 key taxon of semi-desert environments occurring i.e. in sheltered valleys (Walter, 1974), was  
260 also present. AP percentages are low (0–10 %) and mainly composed of *Betula alba*-type and  
261 the dry adapted taxon *Ephedra* with single pollen grains of *Pinus sylvestris*-type and *Pinus*  
262 *sibirica*. The conifer pollen suggests either presence of single conifers in locally favorable spots  
263 in the herbaceous steppe or long-distance pollen transport.



265 **Figure 2 Percentage diagram of Tsambagarav ice core spanning the past 5500 years.** Selected pollen types, fern spores,  
266 and coprophilous fungal spores based on the terrestrial pollen sum. Temperate arboreal summary curve consists of *Fagus*,  
267 *Corylus*, *Quercus* and other temperate arboreal pollen taxa. Hollow curves = 10x exaggeration. Diversity estimation (Hurlbert,  
268 1971) based on a minimum pollen sum of 105 for pollen richness (PRI), evenness-detrended pollen richness (DE-PRI), and  
269 evenness index (PIE). Concentration curves for charcoal, pollen and *Sporormiella* in particles l<sup>-1</sup> and total terrestrial pollen  
270 sum. LPAZ = statistically significant local pollen assemblage zones, dashed lines not statistically significant. Chronology  
271 according to Herren et al. (2013), reference horizons in Fig. 1A.

272

273 Tree pollen percentages reach highest peaks between 3000 and 1800 BC (up to 50 %; LPAZ  
274 TSA-2–TSA-3a; Fig. 2) indicating afforestation pulses in the steppes possibly resulting from  
275 moister and/or warmer conditions. *Betula alba*-type percentages (30 %) as well as tree pollen  
276 concentration peaks around 3000 and 1900 BC hint to periods with propitious environmental  
277 conditions that allowed expansion of the pioneer species. Pollen of the arctic-alpine shrub taxa  
278 *Betula nana*-type and *Salix*, as well as *Juniperus* reaches highest percentages of the entire  
279 record during this phase. This suggests an upward expansion of alpine tundra vegetation to  
280 altitudes higher than 3000 m a.s.l., which is today's upper altitudinal limit of alpine tundra  
281 shrubs such as *Salix glauca* and *Betula nana* ssp. *rotundifolia* in the area (Walter, 1974; Gunin  
282 et al., 2009). The second tree pollen peak between 2400 and 2100 BC is marked by an initial  
283 rise of *Betula alba*-type (20 %) followed by a second phase where pollen percentages of *Pinus*  
284 *sibirica*, *Picea*, *Larix*, *Abies*, and *Alnus viridis* increase, indicating a succession from primary  
285 *Betula pendula*-dominated forests to more diverse secondary forests and green alder thickets  
286 (Fig. 2). The rise of pollen from temperate trees (mainly *Quercus*, *Corylus* and *Fagus*) to 5%  
287 may indicate a stronger influence of southern airmasses since the closest occurrence of these  
288 taxa is in China (Wu & Raven, 1999). The forest expansions coincided with a spread of ferns  
289 (maximum fern spore percentages of the record). This period is further characterized by the  
290 lowest pollen concentrations of the entire record (<2000 grains l<sup>-1</sup>) that indicate diluted  
291 microfossil concentrations possibly caused by higher ice accumulation rates due to moister  
292 environments (Fig. 2, Herren et al., 2013).



294 **Figure 3 Percentage diagram of Tsambagarav ice core for the past millennium.** Selected pollen types, fern spores,  
295 coprophilous fungal spores based on the terrestrial pollen sum. Temperate arboreal summary curve consists of *Fagus*, *Corylus*,  
296 *Quercus* and other temperate arboreal taxa. Hollow curves = 10x exaggeration. Diversity estimation (Hurlbert 1971) based on  
297 a minimum pollen sum of 105 for pollen richness (PRI), evenness-detrended pollen richness (DE-PRI), and evenness index  
298 (PIE). Concentrations of charcoal, SCP (spheroidal carbonaceous particles), pollen, and *Sporormiella* in particles l<sup>-1</sup>. LPAZ =  
299 statistically significant local pollen assemblage zones, dashed line not statistically significant. Chronology, presented <sup>14</sup>C-dates  
300 and reference horizons (volcanic layers, drilling year, and tritium peak) according to Herren et al. (2013).

301

302

303 AP decreases stepwise at ca. 1800 BC, 800 BC, 1100 AD, and 1700 AD (LPAZ TSA-3b–  
304 TSA-5b), pointing to several forest or arboreal vegetation retraction phases in the areas  
305 northwest and north of Tsambagarav. Dry *Stipa-Artemisia* steppe (e.g. Poaceae, *Artemisia*) as  
306 well as desert-steppe communities (e.g. increasing Chenopodiaceae and *Salsola*-type  
307 percentage values, Figs 2–3) expanded. The tree diebacks are defined by LPAZ boundaries  
308 indicating significant shifts in the vegetation around the glacier. A short-term *Pinus sibirica*  
309 pollen increase between 900 and 1100 AD (defined by LPAZ TSA-4) hints to a temporary  
310 establishment of the species in the catchment. Maximum landscape openness was reached after  
311 1700 AD (AP <10 %; Fig. 3). AP rises noticeably during LPAZ TSA-6 (1960–2009 AD) which  
312 is mainly due to increasing *Betula alba*-type and indicates rapid spreads of pioneer trees.

313 The presence of Cerealia-type is interpreted as a primary indicator for farming activities if  
314 associated with other pollen indicative of land use (e.g. *Linum usitatissimum*, *Plantago*  
315 *lanceolata*; Lang, 1994). Association with other adventive pollen (or less ideal apophytes  
316 pollen) is needed, because in entire Eurasia Cerealia-type pollen is occasionally produced by  
317 wild grass species (Beer et al., 2007; Van Zeist et al., 2016), e.g. by *Trisetum spicatum*, a  
318 common wild grass species of the Mongolian mountain steppes (Walter, 1974). Secondary  
319 anthropogenic pollen indicators such as *Rumex crispus* (*R. acetosa*-type), Cichorioideae, *Urtica*  
320 and Liliaceae prefer nutrient enriched former campsites suggesting pastoralism activities,  
321 although they may occasionally also occur naturally on humid and nutrient-rich soils in the  
322 Mongolian Altai (Gunin et al., 2009). Thus, the presence and in particular the combined  
323 increase of these indicators (Fig. 2) might point to land use activities in the Mongolian Altai  
324 after 3500 BC. Cerealia-type pollen occurs regularly after 2000 BC and reaches a maximum  
325 around 1000 AD, often in combination with *Urtica*, *Rumex* and Liliaceae. Cerealia-type pollen

326 rises again around 1700 AD, and after 1700 AD *Urtica*, *Cannabis*-type and *Rumex* percentages  
327 increase indicating intensified pastoralism activities (Gunin et al., 2009).

328 Dung fungal spores of *Sporormiella* are continuously present in large quantities along the  
329 entire record indicating continuous herbivore grazing in the steppes. The *Sporormiella* record  
330 suggests that herbivore grazing activities reached a maximum during the afforestation phase  
331 (20 % around 2200 BC). Increased grazing activity was possibly released by an enhanced  
332 productivity of the steppes related to increasing moisture, or less likely, by favorable (humid)  
333 conditions for fungi growth and spore production. As observed for pollen, *Sporormiella*  
334 concentration values remain low due to increased ice accumulation rates. The *Sporormiella*  
335 concentrations rise slightly after 1600 AD, which might be related to intensified herding  
336 activities over the past centuries.

### 337 **Diversity and ordination analysis**

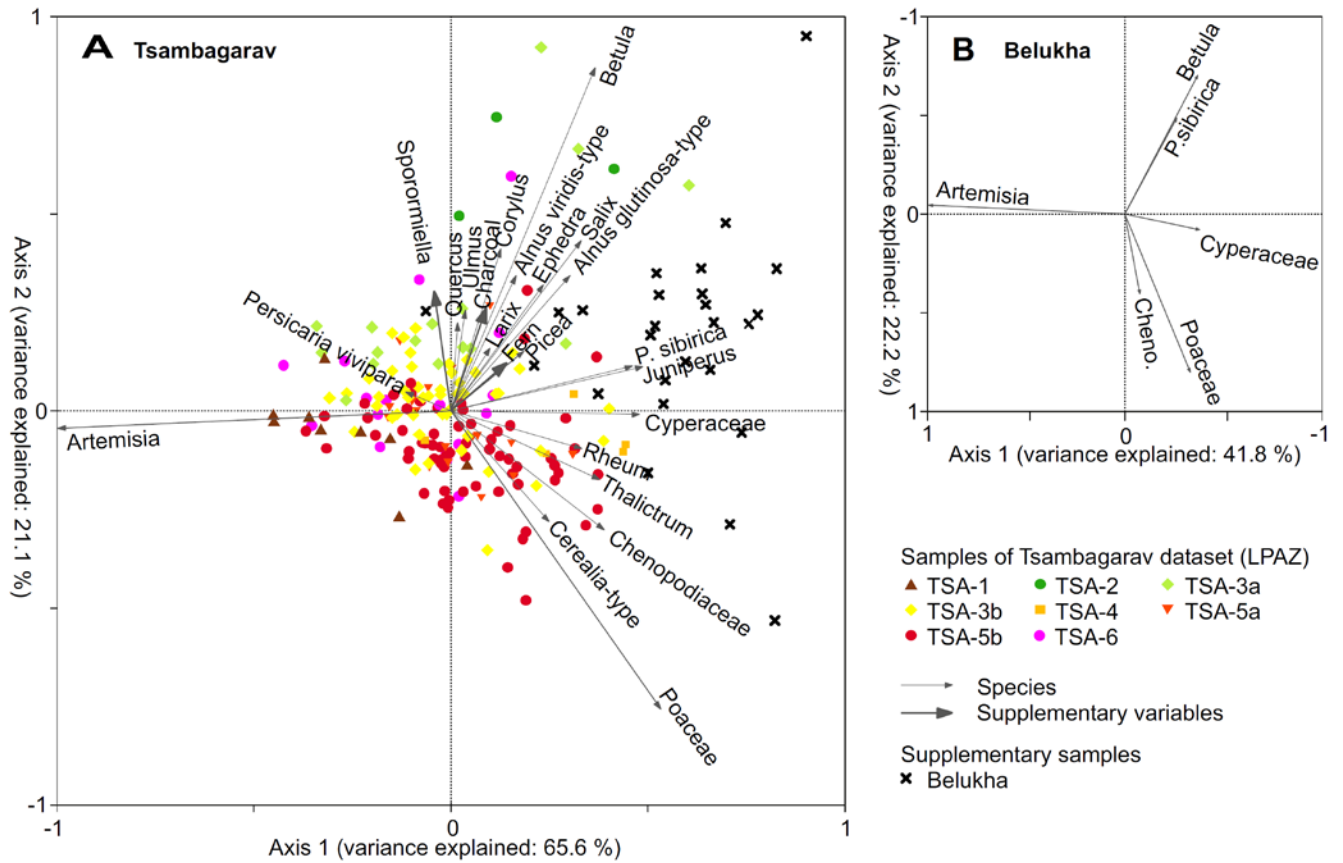
338 In a large pollen catchment such as Tsambagarav that includes a wide range of habitats,  
339 pollen richness is rather related to ecosystem diversity and thus the number of habitats, than to  
340 floristic diversity within plant communities. Low PIE values (<0.5) throughout the sequence  
341 follow PRI suggesting that species evenness was constantly low. However, evenness  
342 reconstructions were possibly affected by the large *Artemisia* portions, a pollen taxon that is  
343 commonly overrepresented in steppic ecosystems (Liu et al., 1999) and prevails over the entire  
344 record (Figs 2–3). PRI and DE-PRI remain low until 3000 BC (PRI ca. 5–15; DE-PRI ca. 10),  
345 followed by an increase (PRI max. 20–30, DE-PRI 15) between 3000 and 2400 BC when AP  
346 percentages are peaking. Given that pollen richness is correlated with AP ( $r = 0.64$ , Figs 2–3)  
347 it is likely that forest expansions contributed to increasing diversity. After the forest retreat at  
348 1800 BC, diversity remained at intermediate levels (PRI ca. 10–20, DE-PRI ca. 10–15) until  
349 1700 AD. Higher diversity in the younger steppes (pre-3000 BC vs. post-1800 BC) was possibly  
350 related to reorganizations to grassy steppe communities (e.g. Poaceae increase; Fig. 3).  
351 Palynological diversity drops to low values after 1700 AD (PRI and DE-PRI around 10)



352 suggesting a further decline of diversity perhaps related to intensified herding (e.g.  
353 *Sporormiella* rise).

354 The sample distribution on the PCA axes 1 and 2 (Fig. 4A) shows a large LPAZ overlap  
355 with only minor vegetation changes over the past five millennia. Samples of LPAZ TSA-1 and  
356 TSA-6 vs. TSA-4 are separated along axis 1 and samples of LPAZ TSA-2 and TSA-3a are  
357 shifted along axis 2, reflecting variations in the vegetation composition between different steppe  
358 communities and boreal forests over time. A very high share (66 %) of the variance is explained  
359 by axis 1 which splits mainly moist steppe communities (*Artemisia*, *Persicaria vivipara*) from  
360 the rest: dry steppic (Chenopodiaceae, *Rheum*, Poaceae), cryophilous alpine *Kobresia*-meadow  
361 (e.g. Cyperaceae) and rather mesophilous boreal forests (e.g. *Betula*, *Pinus sibirica*). Axis 2  
362 explains another 21 % of the variance and separates dry grass steppe (e.g. Poaceae,  
363 Chenopodiaceae, *Thalictrum*) from cryophilous, mesophilous and rather thermophilous  
364 communities: tundra shrublands (e.g. *Alnus viridis*), boreal (*Picea*, *Larix*, *Betula*) and  
365 nemoboreal or temperate (e.g. *Ulmus*, *Quercus*, *Corylus*) arboreal taxa. Thus, both axes may  
366 indicate aspects related to moisture availability and associated temperatures, such as steppic  
367 species composition (e.g. *Artemisia* vs. Chenopodiaceae and Poaceae for axis 1) and biomass  
368 or biome allocation (steppic vs. boreal or nemoboreal) for axis 2.

369 PCA for the Belukha samples (Fig. 4B) reveals that the Tsambagarav results are reproducible  
370 in the Russian Altai. Axis 1 explains 42 % of the variance separating *Artemisia* from dry steppic  
371 *Stipa*-communities (e.g. Poaceae, Chenopodiaceae) and axis 2 explains 22 % separating dry  
372 steppes from boreal forests (*Betula*, *Pinus sibirica*). The compositional similarities between the  
373 two PCA suggests moisture availability and less important temperature as drivers of vegetation  
374 change. If combined (Fig. 4A) Russian Altai sample scores group in one edge of Axis 1, along  
375 an axis 2 gradient. The sample score comparison suggests a high similarity of Belukha with  
376 Tsambagarav during the afforestation phase 3000–1800 BC (TSA-2–TSA-3a). The ordination  
377 clearly separates modern Tsambagarav (TSA-6) and Belukha samples probably because of  
378 moisture-related differences and different anthropogenic influence on both, Mongolian and



380

381 **Figure 4 Principle component analysis (PCA) for pollen percentages of Altai glacier records.** Panel A: PCA for the  
 382 Mongolian Altai (Tsambagarav glacier) today surrounded by open steppes with only relict forest patches, spanning 3500 BC–  
 383 2009 AD. Sample scores with different symbols for the corresponding local pollen assemblage zone (LPAZ), selected species  
 384 scores (black arrows corresponding to pollen types) indicate vegetation composition changes for sample scores from boreal  
 385 forest (e.g. *Pinus cembra*) to less dry (e.g. *Artemisia*) and arid steppes (e.g. *Chenopodiaceae*). Selected supplementary variables  
 386 (grey arrows, *Sporormiella* and fern spores as percentages of the terrestrial pollen sum [%], charcoal concentrations [particles  
 387 l<sup>-1</sup>]). Russian Altai (Belukha glacier) today surrounded by abundant boreal forests spanning 1250–2001 AD. Sample scores are  
 388 plotted as supplementary data not influencing the ordination (black cross symbols). The PCA results underline the similarity  
 389 of mid-Holocene forest communities in the Mongolian Altai with historical and modern boreal forests in the Russian Altai.  
 390 Panel B: Selected species scores for the Belukha dataset. Selected species scores for the Russian Altai show a close relationship  
 391 with species scores from the Mongolian Altai (Panel A). Taken together this finding underscores the vulnerability of extant  
 392 Central Asian forests to current and future climate change. Specifically, future vegetation dynamics in the Russian Altai may  
 393 follow past climate impact trajectories in the Mongolian Altai, from forested (positive scores) to steppic communities (negative  
 394 scores) along PCA axis 1.

## 395 **Fire and industrial pollution history**

396 The average charcoal concentration in the upper firm (ca. 6000 particles l<sup>-1</sup> for the period  
397 2009–2005 AD) corresponds to a microscopic charcoal influx of ca. 200 particles cm<sup>-2</sup> year<sup>-1</sup>  
398 or 0.085 mm<sup>2</sup> cm<sup>-2</sup> year<sup>-1</sup> (Tinner & Hu, 2003), which is extremely low if compared to sediment  
399 records (Adolf et al., 2017). Charcoal concentrations reveal no major fire activity trend between  
400 3500 BC and 1700 AD with an average of ~5000 particles l<sup>-1</sup>. A single outstanding charcoal  
401 peak around 1540 BC (29'000 particles l<sup>-1</sup>) suggests a short phase of major fire activity ca. 250  
402 years after a major forest decline. Other charcoal-concentration inferred fire-activity peaks  
403 (>90-percentile = >7300 particles l<sup>-1</sup>; Figs 2–3) also occurred following forest declines (e.g.  
404 ~2650 BC ca. 150 years after the forest decline around 2800 BC), suggesting that collapses of  
405 boreal taxa provided dead biomass and thus fuel for fire activity (De Groot et al., 2000; Eichler  
406 et al., 2011; Tinner et al., 2015; Kuuluvainen et al., 2017). Charcoal concentrations remain low  
407 after 1700 AD with an average of ~2600 particles l<sup>-1</sup> and no peaks >90-percentile indicating  
408 minimal fire activity when herbaceous steppe ecosystems were dominant. However,  
409 microscopic charcoal hints to minor increase of fire activity after 1960 AD. Charcoal  
410 concentration as supplementary variable in the PCA (Fig. 4) groups with AP, again suggesting  
411 biomass availability as an important factor for burning.

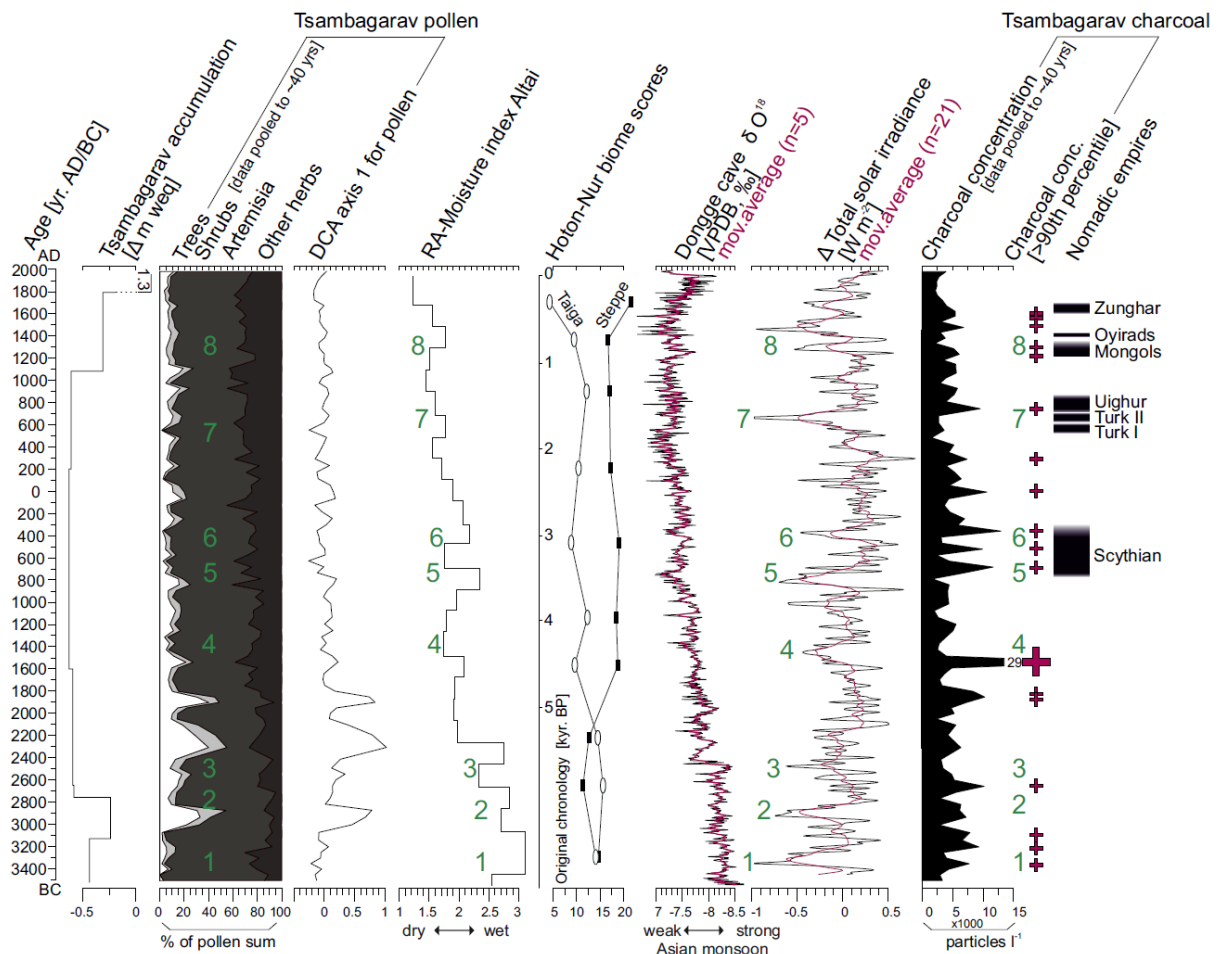
412 First SCP occur around ca. 1720 AD at the beginning of zone TSA-5b (Fig. 3). Those  
413 scattered but frequent particles indicate initial atmospheric pollution, possibly deriving from  
414 early industrialization and mining activities (Naumov, 2006). Regionally, they coincide with  
415 minimum fire activity and maximum landscape openness, indicating a possible shift from solely  
416 timber-based to increasingly fossil fuel-based energy consumption, perhaps motivated by  
417 limited timber availability. SCP rise after 1920 AD, suggesting amplified industrial air pollution  
418 during the 20<sup>th</sup> century. A first concentration peak around 1960 AD with 80 particles l<sup>-1</sup> and a  
419 second maximum around 2000 AD (100 particles l<sup>-1</sup>) coincide with highest charcoal  
420 concentration values (6000 particles l<sup>-1</sup>) during the 20<sup>th</sup> century.

## 421 **DISCUSSION**

### 422 **Fire and fuel dynamics during the past 5000 years**

423 Tsambagarav receives ca. 200 microscopic charcoal particles  $\text{cm}^{-2} \text{yr}^{-1}$  today which is in the  
424 same order of magnitude as Belukha glacier 320 km northwest in the Russian Altai (150  
425 particles  $\text{cm}^{-2} \text{yr}^{-1}$ ; Eichler et al., 2011) at a similar altitude (4062 m a.s.l.). Charcoal influx  
426 values at Belukha are ca. 40 times lower than at nearby Teletskoye Lake at 1900 m a.s.l. (8200  
427 particles  $\text{cm}^{-2} \text{yr}^{-1}$ ; Andreev et al., 2007). The influx difference between glaciers and  
428 neighboring lake sediment archives is best explained by the remoteness of the glaciers and the  
429 limited vertical atmospheric transport to the high elevation ice core sites (Gilgen et al., in  
430 review). To our knowledge, no microscopic charcoal records from the Mongolian Altai are  
431 available. Local fire reconstructions are based on macroscopic charcoal and cover the past  
432 millennia (Umbanhowar et al., 2009; Unkelbach et al., 2018). Despite the spatio-temporal  
433 variability their reconstructed fire signal corresponds to our regional fire activity peaks from  
434 Tsambagarav (microscopic charcoal peaks >90-percentile, Fig. A1), if dating uncertainties are  
435 considered. Recent calibration studies at the continental scale showed that micro- and  
436 macroscopic charcoal has very similar spatial proveniences spanning a radius of about 40 km  
437 around sedimentary sites (Adolf et al., 2017). Glaciers on the other hand act as a regional to  
438 subcontinental archive of biomass burning, integrating fire activity over larger spatial scales  
439 (Legrand et al., 2016). Very high concentrations >20.000 particles  $\text{l}^{-1}$  suggest that the fire  
440 activity peak in the Tsambagarav record around 1500 BC was comparable to the maximum  
441 burning of the past 800 years that occurred around 1600 AD at Belukha glacier in the Russian  
442 Altai (Fig. A2). The 1500 BC maximum fire phase in the Tsambagarav record may  
443 chronologically correspond to the late-Holocene fire activity peak at Zagas Nur around 20 km  
444 southwest of Tsambagarav (Umbanhowar et al., 2009) where it is dated to 1400 BC, while at  
445 Doroo Nur (50 km south) fire activity was only moderate around 1500 BC. As the fire peak  
446 does not occur in more distant records from western Mongolia (Fig. A1; Umbanhowar et al.,

447 2009) we assume that the fire might have been localized close to the glacier (20–40 km) or  
 448 located north or northwest.



449

450 **Figure 5 Comparison of the palynological record from Tsambagarav with regional and climate records.** From left:  
 451 Tsambagarav ice accumulation rate (anomaly from the mean of the past 6000 years, Herren et al., 2013), Tsambagarav  
 452 vegetation reconstruction (summary curve for pollen, DCA-axis 1, correlation arboreal pollen percentages : DCA scores axis  
 453 1:  $r = 0.95$ ; this study), regionally-averaged moisture index for the Altai Mountains based on pollen records (Wang & Feng,  
 454 2013), biome scores from Hoton Nur with original chronology adjusted (Tarasov et al., 2000; Rudaya et al., 2009), Asian  
 455 monsoon reconstruction from Dongge cave (Wang et al., 2005), solar activity fluctuation reconstruction based on  $^{10}\text{Be}$   
 456 measurements in polar ice (Steinilber et al., 2009), Tsambagarav fire reconstruction (charcoal concentrations, this study) and  
 457 selected nomadic empires (Rogers, 2012). Green numbers indicate climatically induced forest minima phases at Tsambagarav.

458

459 Increased fire activity at Tsambagarav was related to declines of boreal tree stands or forests  
 460 that likely provided fuel for burning (Fig. 5), similarly to what was found at Belukha (Eichler  
 461 et al., 2011). There, a dry period inducing forest diebacks was succeeded by maximum fire  
 462 activity around 1600 AD (Fig. A2), a period with increased fire activity also in the Tsambagarav  
 463 area (three consecutive charcoal peaks  $>90$ -percentile; Fig. 5) and in the Eurasian Arctic  
 464 (Akademii Nauk ice record; Griemann et al., 2017). Lacking biomass availability combined  
 465 with low temperatures during the Little Ice Age period may explain the fire minimum at 1700–

466 1960 AD when maximum vegetation openness is documented in the pollen record of  
467 Tsambagarav and at adjacent sites (Fig. 5; Umbanhowar et al., 2009, Unkelbach et al., 2018).  
468 Finally, the past four decades of the Tsambagarav record suggest again a slight increase of  
469 regional and local fire activity possibly caused by increased biomass availability due to pioneer  
470 birch forest expansions.

#### 471 **Composition, successional dynamics and diebacks of the mid-Holocene forests**

472 Our high-resolution record from Tsambagarav provides a unique chronological control in  
473 combination with high-temporal and continuous sampling resolution and is therefore suited to  
474 assess rapid ecosystem responses to climate change. The Tsambagarav record suggests that the  
475 Mongolian Altai experienced several prominent forest contraction and expansion phases before  
476 1800 BC. The magnitude and fluctuation pattern of this early phase are comparable to the  
477 pattern observed for the past 800 years in the Russian Altai (Eichler et al., 2011). There, mixed  
478 *Pinus sibirica-Larix sibirica* stands form a dense forest belt between 1000 m a.s.l. and the  
479 timberline around 2000 m a.s.l. in which *Abies sibirica* and *Picea obovata* co-occur in areas  
480 where soil moisture is sufficient (Eichler et al., 2011). Below this belt *Betula pendula* and *Pinus*  
481 *sylvestris* form boreal forests (Walter, 1974). The forests in the Russian Altai produce a pollen  
482 signal which is comparable to that of the Tsambagarav record during the period 3000–1800 BC  
483 (Figs 4 and A2). The Belukha pollen assemblage is mainly composed of *Pinus sibirica* and  
484 *Betula* with only single *Larix* grains despite its importance in the vegetation (Eichler et al.,  
485 2011). Scattered *Larix* pollen in the Tsambagarav record may thus suggest that *Larix sibirica*  
486 was an important forest element during the afforestation phases in the Mongolian Altai. This  
487 similarity is striking, given that nowadays *Larix sibirica* and *Pinus sibirica* form only relict and  
488 discontinuous forest belts in the northern part of the Mongolian Altai and *Abies sibirica* has  
489 completely vanished (Walter, 1974; Gunin et al., 2009).

490 The multiproxy Belukha record suggests that forest diebacks in the Russian Altai were  
491 induced by severe drought decades resulting in enhanced fire risk and that forests recovered

492 rapidly after moisture re-increased (Eichler et al., 2011). The repeated forest contractions at  
493 Tsambagarav followed by *Artemisia* steppe expansions indicate similar vegetation responses to  
494 moisture variability. Forest recoveries similar to the Russian Altai ended 1800 BC. This is in  
495 line with regional sedimentary pollen records showing consistent deforestation in the  
496 Mongolian Altai during the mid- to late-Holocene. For instance, pollen-inferred vegetation  
497 reconstructions from Hoton Nur point to taiga forest contractions between 3000–2000 BC (Fig.  
498 5; Rudaya et al., 2009) to never recover again. At Bayan Nur forests contracted around 1500  
499 BC, in the Dayan Nur region around 650 BC and in the Achit Nur area between 4000 BC and  
500 200 AD (Gunin et al., 2009; Sun et al., 2013; Unkelbach et al., 2018). Diachronic forest  
501 diebacks suggest that moisture thresholds for forest growth were underrun in different periods  
502 in the Mongolian Altai. Specifically, local forest persistence until about 800 BC, 1200 AD and  
503 1700 AD indicates that decreasing moisture effects on forests endured until modern times,  
504 resulting in stepwise forest and tree stand disruptions. These late-Holocene dynamics occurred  
505 also at larger distances, e.g. at Akkol Lake (ca. 190 km) in the northern Tuva region after 1000  
506 BC (Blyakharchuk et al., 2004; Fig. 1A) suggesting that forests contracted also far north of the  
507 Mongolian Altai in response to moisture reductions. However, chronological uncertainties as  
508 resulting from few <sup>14</sup>C-dates from bulk sediments (see Rey et al., 2018) and a general lack of  
509 <sup>14</sup>C-dates in the mid- to late-Holocene (Gunin et al., 2009; Sun et al., 2013) impede precise  
510 assessments of the deforestation timing at individual sites.

### 511 **Climate-driven pulses of steppe expansions and human impact after 1800 BC**

512 Hunter and gatherer communities inhabited the Altai region since the early-Holocene  
513 (Volkov, 1995; Hauck et al., 2012), and nomadic herders were present since at least 1000 BC  
514 (Fig. 5; Fernández-Giménez, 1999; Rogers, 2012; Rudaya et al., 2008), but their impact on the  
515 natural vegetation is supposed to be minor (Bourgeois et al., 2007; Rudaya et al., 2009). We  
516 thus assume that natural climate change, such as aridity and/or cooling, was the main forcing  
517 of repeated forest contractions and subsequent herbaceous steppes expansions during the late-

518 Holocene (Schlütz et al., 2008). A pollen-based moisture index derived from other sites in the  
519 Mongolian Altai (Wang & Feng, 2013) was previously interpreted as a proxy for the Asian  
520 summer monsoon strength (Fig. 5). This index is driven by the same factors as our pollen data  
521 and is therefore not an independent climatic proxy and indeed its course is in line with our  
522 ecological interpretation, thus indicating similar moisture trends across sites. The vegetation-  
523 based reconstructions are in good agreement with mid-Holocene climate model simulations for  
524 Asian monsoon strength (Harrison et al., 2016) and with pollen-independent oxygen isotope  
525 records (e.g. Dongge cave record; Fig. 5; Wang et al., 2005; Wang & Feng, 2013) that suggest  
526 declining moisture availability in the Mongolian Altai in response to a weakening of monsoon  
527 activity resulting from changes of orbital forcing during the late-Holocene. Reduced monsoon  
528 sources of moisture as a possible cause for deforestation at Hoton Nur was proposed by Rudaya  
529 et al. (2009). Although our Tsambagarav vegetation and fire record begins at 3500 BC when  
530 monsoon had already started to weaken (Wang et al., 2005), we assume that the progressive  
531 late-Holocene reduction of subtropical air-masses resulted in strong moisture oscillations that  
532 may have resulted in flickering of forest ecosystems before their final collapse at ca. 1800 BC  
533 (Dakos et al., 2013).

534 The Tsambagarav record suggests that the long-term tree contraction in the Mongolian Altai  
535 continued stepwise after 1800 BC to reach its apex only 300–200 years ago. Contractions of  
536 forest ecosystems were possibly induced by climate variability related to e.g. solar activity  
537 changes (Eichler et al., 2009; Steinhilber et al., 2009; Roth & Joos, 2013). For instance, the  
538 forest minima around 3400 BC, 2800 BC, 2500 BC, 800–400 BC, 500 AD, and 1200 AD might  
539 have been related to dry cooling events (Fig. 5) as partly recorded regionally (e.g. the 4.2 kyr  
540 cool and dry period, Staubwasser & Weiss, 2006; Dixit et al., 2014), in other Northern  
541 Hemisphere records from the Alpine region and Alaska (Haas et al., 1998; Tinner et al., 2015)  
542 or in the reconstructed global surface air temperature (Roth & Joos, 2013).

543 During the past decades, climate proxies suggest reversing climate trends with warming (e.g.  
544 Eichler et al., 2009; Roth & Joos, 2013) and re-strengthening of the Asian monsoon (e.g.



545 reconstructed from Dongge cave isotope record; Wang et al., 2005). In contrast, after the end  
546 of the Little Ice Age at ca. 1850 AD (Eichler et al., 2011) tree stands in the Mongolian Altai did  
547 not recover suggesting a decoupling of vegetation dynamics from climate, e.g. due to increasing  
548 human activities. The historical onset of larger-scale smelting in the Altai dates to 1729 AD  
549 (Naumov, 2006) coinciding with the beginning of the industrial pollution signal in our ice  
550 record as documented in SCPs (Fig. 3). The related energy requirements induced increasing  
551 human pressure not only on the Russian Altai forests but also on the remaining tree stands in  
552 the Mongolian Altai until 1960 AD (Lkhagvadorj et al., 2013), likely shifting the lower tree  
553 line upwards (Dulamsuren et al., 2014). Thus, human activities altered vegetation responses to  
554 climate. The Tsambagarav record suggests that industrial pollution remained high after 1960  
555 AD and only pioneer *Betula pendula* may have very recently recovered, when fossil fuel-based  
556 energy consumption (e.g. coal or diesel-consuming engines for heating, transportation or water-  
557 supply) increased, relieving pressure on woody stands (Fernández-Giménez, 1999).

#### 558 **Altai ecosystems under future climate change**

559 Past vegetation dynamics suggest that warmer and moister conditions during the mid-  
560 Holocene allowed boreal forest establishments in the Tsambagarav area in the Mongolian Altai.  
561 These forests collapsed around 1800 BC. Subsequently, further stepwise tree reductions and a  
562 gradual shift to more dry adapted steppe communities occurred likely in response to drying and  
563 cooling during the late-Holocene. Future climate projections for continental areas propose  
564 further warming and drying in the coming decades for the Altai Region (Sato, Kimura, & Kitoh,  
565 2007; Tchebakova, Blyakharchuk, & Parfenova, 2009; Dai, 2011; Collins et al., 2013;  
566 Dulamsuren, Khishigjargal, Leuschner, & Hauck, 2014; IPCC, 2014; Lehner et al., 2017). In  
567 agreement, during the past decades, the Mongolian Altai experienced significant warming and  
568 increasing numbers of drought periods. Precipitation more often included heavy rainfall events  
569 that are only partly beneficial for vegetation (D'Arrigo et al., 2001; Dulamsuren, Hauck, &  
570 Leuschner 2010; Lkhagvadorj, Hauck, Dulamsuren, & Tsogtbaatar, 2013). Other areas in

571 Mongolia and southern Siberia also experienced climate warming and moisture decrease,  
572 probably affecting tree growth and hindering forest regeneration (Allen et al., 2010;  
573 Tsogtbaatar, 2013; Dulamsuren, Khishigjargal, Leuschner, & Hauck, 2014; Xu et al., 2017). If  
574 future climate projections are correct about declining moisture availability, the persisting forest  
575 patches and belts in the Mongolian, Russian Altai and other dry areas of Central Asia will be  
576 strongly affected. For instance, forest boundaries might shift north of the Russian Altai  
577 releasing unprecedented forest collapses in response to increasing drought. The available fire  
578 histories from ice core records from the Russian and Mongolian Altai also suggest that fire  
579 incidence may increase where biomass is not limiting burning (Eichler et al., 2011; Hessler et al.,  
580 2016). This interpretation of the paleo record agrees with modern observations indicating a  
581 significant link between dry conditions and fire activity (Tsogtbaatar, 2013; Ponomarev &  
582 Kharuk, 2016). Thus, fire may exacerbate the effects of future climate change on vegetation,  
583 especially if associated to high grazing pressure (Tsogtbaatar, 2004; Hauck et al., 2014;  
584 Ponomarev & Kharuk, 2016).

585 In the past, when climate forcing was natural, warm conditions were in this region usually  
586 accompanied by increases in moisture availability, likely deriving from increased monsoonal  
587 and/or westerly wind activity that promoted forest growth. Despite many projection efforts and  
588 progresses, the magnitude of global warming and in particular of precipitation changes remains  
589 ambiguous (Braconnot et al., 2012). Future projections may underestimate moisture availability  
590 in continental areas (Berg, Sheffield, & Milly, 2017), as for example, northern hemisphere  
591 monsoon simulations for the mid-Holocene underestimate its magnitude (Braconnot et al.,  
592 2012; Harrison et al., 2015). If moisture should unexpectedly increase with future warming as  
593 it did during the early and mid late-Holocene, forests may thus persist and perhaps even expand  
594 in the Mongolian Altai, as they did during the period 3000–1800 BC, at least if human pressure  
595 will not become excessive.

596 **CONCLUSIONS**

597 The Tsambagarav record demonstrates for the first time the ecological potential of ice  
598 palynology, specifically, based on its high chronological resolution and precision, it provides  
599 novel insights into past fire, vegetation, and land use dynamics in the Mongolian Altai region.  
600 Late-Holocene vegetation reorganizations in response to climate and moisture availability  
601 changes underscore the vulnerability of forest ecosystems that are still thriving in the  
602 Mongolian or Russian Altai. We conclude that precipitation regime changes were the main  
603 driver for forest diebacks ca. 4700–4000 years ago and their final collapse ca. 3800 years ago.  
604 The lacking resilience of forest communities (e.g. *Pinus sibirica-Larix sibirica* stands) to  
605 moisture changes emphasizes the vulnerability of forests in other dry areas of Central Asia, if  
606 global warming will be associated to moisture declines as anticipated by future scenarios (IPCC,  
607 2014). To better assess past vegetation and forest fire dynamics, new high-resolution and -  
608 precision multiproxy studies from natural archives are urgently needed. Such studies may help  
609 to disclose the mechanisms and processes behind the vulnerability of plant species and  
610 communities. Ultimately, they are thus essential to improve our knowledge of future ecosystem  
611 responses to global change.

612 **ACKNOWLEDGMENTS**

613 We are grateful to Ch.E. Umbanhowar for providing macroscopic charcoal data, to J.F.N.  
614 van Leeuwen for assistance with rare pollen type analysis, to J. Unkelbach from University of  
615 Göttingen for valuable discussions, to the Russian Federation for support with the international  
616 drilling campaign, and to the ice drilling crew. We thank H. Behling and an anonymous  
617 reviewer for constructive remarks that substantially improved the manuscript. We acknowledge  
618 the Sinergia project Paleo fires from high-alpine ice cores funded by the Swiss National Science  
619 Foundation (SNF grant 154450).

620 **DATA AVAILABILITY**

621 All data will be deposited in the Alpine Palynological Database (ALPADABA) and the  
622 Neotoma database ([www.neotomadb.org](http://www.neotomadb.org)).

623 **REFERENCES**

- 624 Adolf, C., Wunderle, C., Colombaroli, C., Weber, H., Gobet, E., Heiri, O., van Leeuwen, J. F.  
625 N., Bigler, C., Connor, S. E., Gařka, M., La Mantia, T., Makhortykh, S., Svitavská-  
626 Svobodová, H., Vanničre, B., & Tinner, W. (2017). The sedimentary and remote-sensing  
627 reflection of biomass burning in Europe. *Global Ecology and Biogeography*, 27, 199-212.  
628 <https://doi.org/10.1111/geb.12682>
- 629 Allen, C. D., Macalady, A. K., Chenchouni, H., Bachelet, D., McDowell, N., Vennetier, M.,  
630 Kitzberger, T., Rigling, A., Breshears, D. D., Hogg, E. H., Gonzalez, P., Fensham, R., Zhang,  
631 Z., Castro, J., Demidova, N., Lim, J.-H., Allard, G., Running, S. W., Semerci, A., & Cobb,  
632 N. (2010). A global overview of drought and heat-induced tree mortality reveals emerging  
633 climate change risks for forests. *Forest ecology and management*, 259(4), 660-684.  
634 <https://doi.org/10.1016/j.foreco.2009.09.001>
- 635 Andreev, A. A., Pierau, R., Kalugin, I. A., Daryin, A. V., Smolyaninova, L. G., & Diekmann,  
636 B. (2007). Environmental changes in the northern Altai during the last millennium  
637 documented in Lake Teletskoye pollen record. *Quaternary Research*, 67(3), 394-399.  
638 <https://doi.org/10.1016/j.yqres.2006.11.004>
- 639 Beer, R., Heiri, O., & Tinner, W. (2007). Vegetation history, fire history and lake development  
640 recorded for 6300 years by pollen, charcoal, loss on ignition and chironomids at a small lake  
641 in southern Kyrgyzstan (Alay Range, Central Asia). *The Holocene*, 17(7), 977-985.  
642 <https://doi.org/10.1177/0959683607082413>
- 643 Bennett, K. D. (1996). Determination of the number of zones in a biostratigraphical sequence.  
644 *New Phytologist*, 132(1), 155-170. <https://doi.org/10.1111/j.1469-8137.1996.tb04521.x>
- 645 Berg, A., Sheffield, J., & Milly, P. C. (2017). Divergent surface and total soil moisture  
646 projections under global warming. *Geophysical Research Letters*, 44(1), 236-244.  
647 <https://doi.org/10.1002/2016GL071921>
- 648 Beug, H.-J. (2004). 2004: Leitfaden der Pollenbestimmung für Mitteleuropa und angrenzende  
649 Gebiete. Munich: Pfeil.
- 650 Birks, H.-J. (1968). The identification of *Betula nana* pollen. *New Phytologist*, 67(2), 309-314.  
651 <https://doi.org/10.1111/j.1469-8137.1968.tb06386.x>
- 652 Birks, H. J. B., & Gordon, A. (1985). Numerical Methods in Quaternary Pollen Analysis.  
653 London: Academic Press.
- 654 Birks, H. J. B., & Line, J. M. (1992). The use of rarefaction analysis for estimating  
655 palynological richness from Quaternary pollen-analytical data. *The Holocene*, 2(1), 1-10.  
656 <https://doi.org/10.1177/095968369200200101>
- 657 Blyakharchuk, T. A., Wright, H. E., Borodavko, P. S., van der Knaap, W. O., & Ammann, B.  
658 (2004). Late Glacial and Holocene vegetational changes on the Ulagan high-mountain

- 659 plateau, Altai Mountains, southern Siberia. *Palaeogeography, Palaeoclimatology,*  
660 *Palaeoecology*, 209(1), 259-279. <https://doi.org/10.1016/j.palaeo.2004.02.011>
- 661 Bourgeois, J., De Wulf, A., Goossens, R., & Gheyle, W. (2007). Saving the frozen scythian  
662 tombs of the altai mountains (Central Asia). *World Archaeology*, 39(3), 458-474.
- 663 Braconnot, P., Harrison, S. P., Kageyama, M., Bartlein, P. J., Masson-Delmotte, V., Abe-Ouchi,  
664 A., Otto-Bliesner, B., & Zhao, Y. (2012). Evaluation of climate models using palaeoclimatic  
665 data. *Nature Climate Change*, 2(6), 417. doi:10.1038/nclimate1456
- 666 Brugger, S. O., Gobet, E., Schanz, F., Heiri, O., Schwörer, C., Sigl, M., Schwikowski, M., &  
667 Tinner, W. (2018). A quantitative comparison of microfossil extraction methods from ice  
668 cores. *Journal of glaciology*, 64(245), 432-442. <https://doi.org/10.1017/jog.2018.31>
- 669 Clegg, B. F., Tinner, W., Gavin, D. G., & Hu, F. S. (2005). Morphological differentiation of  
670 *Betula* (birch) pollen in northwest North America and its palaeoecological application. *The*  
671 *Holocene*, 15(2), 229-237. <https://doi.org/10.1191/0959683605hl788rp>
- 672 Collins, M., R. Knutti, J. Arblaster, J.-L. Dufresne, T. Fichet, P. Friedlingstein, X. et al.  
673 (2013). Long-term Climate Change: Projections, Commitments and Irreversibility. In:  
674 Climate Change 2013: The Physical Science Basis. Contribution of Working Group I to the  
675 Fifth Assessment Report of the Intergovernmental Panel on Climate Change [Stocker, T.F.,  
676 D. Qin, G.-K. Plattner, M. Tignor, S.K. Allen, J. Boschung, A. et al. (eds.)]. Cambridge  
677 University Press, Cambridge, United Kingdom and New York, NY, USA.
- 678 Colombaroli, D., & Tinner, W. (2013). Determining the long-term changes in biodiversity and  
679 provisioning services along a transect from Central Europe to the Mediterranean. *The*  
680 *Holocene*, 23(11), 1625-1634. <https://doi.org/10.1177/0959683613496290>
- 681 Conedera, M., Tinner, W., Neff, C., Meurer, M., Dickens, A. F., & Krebs, P. (2009).  
682 Reconstructing past fire regimes: methods, applications, and relevance to fire management  
683 and conservation. *Quaternary Science Reviews*, 28(5), 555-576.  
684 <https://doi.org/10.1016/j.quascirev.2008.11.005>
- 685 Dai, A. (2011). Drought under global warming: a review. *Wiley Interdisciplinary Reviews:*  
686 *Climate Change*, 2(1), 45-65. <https://doi.org/10.1002/wcc.81>
- 687 Dakos, V., van Nes, E. H., & Scheffer, M. (2013). Flickering as an early warning signal.  
688 *Theoretical Ecology*, 6(3), 309-317. <https://doi.org/10.1007/s12080-013-0186-4>
- 689 D'Arrigo, R., Jacoby, G., Frank, D., Pederson, N., Cook, E., Buckley, B., Nachin, B., Mijiddorj,  
690 R., & Dugarjav, C. (2001). 1738 years of Mongolian temperature variability inferred from a  
691 tree-ring width chronology of Siberian pine. *Geophysical Research Letters*, 28(3), 543-546.  
692 <https://doi.org/10.1029/2000GL011845>
- 693 De Groot R. C., Woodward B., & Hennon P. E. (2000). Natural decay resistance of heartwood  
694 from dead, standing yellow-cedar trees: laboratory evaluations. *Forest Product Journal* 50,  
695 53-59.
- 696 Dixit, Y., Hodell, D. A., & Petrie, C. A. (2014). Abrupt weakening of the summer monsoon in  
697 northwest India~ 4100 yr ago. *Geology*, 42(4), 339-342 <https://doi.org/10.1130/G35236.1>
- 698 Dulamsuren, C., Hauck, M., & Leuschner, C. (2010). Recent drought stress leads to growth  
699 reductions in *Larix sibirica* in the western Khentey, Mongolia. *Global Change Biology*,  
700 16(11), 3024-3035. <https://doi.org/10.1111/j.1365-2486.2009.02147.x>

- 701 Dulamsuren, C., Klinge, M., Degener, J., Khishigjargal, M., Chenlemuge, T., BatEnerel, B.,  
702 Yeruult, Y., Saindovdon, D., Ganbaatar, K., Tsogtbaatar, J., Leuschner, C., & Hauck, M.  
703 (2016). Carbon pool densities and a first estimate of the total carbon pool in the Mongolian  
704 forest-steppe. *Global change biology*, 22(2), 830-844. <https://doi.org/10.1111/gcb.13127>
- 705 Dulamsuren, C., Khishigjargal, M., Leuschner, C., & Hauck, M. (2014). Response of tree-ring  
706 width to climate warming and selective logging in larch forests of the Mongolian Altai.  
707 *Journal of Plant Ecology*, 7(1), 24-38. <https://doi.org/10.1093/jpe/rtt019>
- 708 Eichler, A., Tinner, W., Brüttsch, S., Olivier, S., Papina, T., & Schwikowski, M. (2011). An ice-  
709 core based history of Siberian forest fires since AD 1250. *Quaternary Science Reviews*,  
710 30(9), 1027-1034. <https://doi.org/10.1016/j.quascirev.2011.02.007>
- 711 Eichler, A., Olivier, S., Henderson, K., Laube, A., Beer, J., Papina, T., Gäggeler, H. W., &  
712 Schwikowski, M. (2009). Temperature response in the Altai region lags solar forcing.  
713 *Geophysical Research Letters*, 36(1). <https://doi.org/10.1029/2008GL035930>
- 714 Fernández-Giménez, M. E. (1999). Sustaining the steppes: a geographical history of pastoral  
715 land use in Mongolia. *Geographical Review*, 89(3), 315-342. <https://doi.org/10.2307/216154>
- 716 Finsinger, W., & Tinner, W. (2005). Minimum count sums for charcoal concentration estimates  
717 in pollen slides: accuracy and potential errors. *The Holocene*, 15(2), 293-297.  
718 <https://doi.org/10.1191/0959683605hl808rr>
- 719 Gilgen, A., Adolf, C., Brugger, S. O., Ickes, L., Schwikowski, M., van Leeuwen, J. F. N.,  
720 Tinner, W., & Lohmann, U. (in review). Implementing Microscopic Charcoal Particles into  
721 a Global Aerosol-Climate Model. <https://doi.org/10.5194/acp-2017-1116>
- 722 Golan-Goldhirsh, A. (2009). Bridging the gap between ethnobotany and biotechnology of  
723 Pistacia. *Israel journal of plant sciences*, 57(1-2), 65-78.
- 724 Grieman, M. M., Aydin, M., Fritzsche, D., McConnell, J. R., Opel, T., Sigl, M., & Saltzman,  
725 E. S. (2017). Aromatic acids in a Eurasian Arctic ice core: a 2600-year proxy record of  
726 biomass burning. *Climate of the Past*, 13(4), 395. <https://doi.org/10.5194/cp-13-395-2017>
- 727 Gunin, P. D., Vostokova, E. A., Dorofeyuk, N. I., Tarasov, P. E., & Black, C. C. (Eds.). (1999).  
728 Vegetation Dynamics of Mongolia. Dordrecht: Kluwer Academic Publishers.
- 729 Haas, J. N., Richoz, I., Tinner, W., & Wick, L. (1998). Synchronous Holocene climatic  
730 oscillations recorded on the Swiss Plateau and at timberline in the Alps. *The Holocene*, 8(3),  
731 301-309. <https://doi.org/10.1177/0959683607082413>
- 732 Harrison, S. P., Bartlein, P. J., & Prentice, I. C. (2016). What have we learnt from palaeoclimate  
733 simulations?. *Journal of Quaternary Science*, 31(4), 363-385.  
734 <https://doi.org/10.1002/jqs.2842>
- 735 Harrison, S. P., Bartlein, P. J., Izumi, K., Li, G., Annan, J., Hargreaves, J., Braconnot, P., &  
736 Kageyama, M. (2015). Evaluation of CMIP5 palaeo-simulations to improve climate  
737 projections. *Nature Climate Change*, 5(8), 735. <https://doi.org/10.1038/nclimate2649>
- 738 Hauck, M., Dulamsuren, C., Bayartogtokh, B., Ulykpan, K., Burkitbaeva, U. D., Otgonjargal,  
739 E., Titov, S. V., Enkhbayar, T., Sundetpaev, A. K., Beket, U., & Leuschner, C. (2014).  
740 Relationships between the diversity patterns of vascular plants, lichens and invertebrates in  
741 the Central Asian forest-steppe ecotone. *Biodiversity and conservation*, 23(5), 1105-1117.  
742 <https://doi.org/10.1007/s10531-014-0648-z>

- 743 Hauck, M., Javkhlan, S., Lkhagvadorj, D., Bayartogtokh, B., Dulamsuren, C., & Leuschner, C.  
744 (2012). Edge and land-use effects on epiphytic lichen diversity in the forest-steppe ecotone  
745 of the Mongolian Altai. *Flora-Morphology, Distribution, Functional Ecology of Plants*,  
746 207(6), 450-458. <https://doi.org/10.1016/j.flora.2012.03.008>
- 747 Heiri, O., & Lotter, A. F. (2001). Effect of low count sums on quantitative environmental  
748 reconstructions: an example using subfossil chironomids. *Journal of Paleolimnology*, 26(3),  
749 343-350. <https://doi.org/10.1023/A:1017568913302>
- 750 Henne, P. D., Elkin, C. M., Reineking, B., Bugmann, H., & Tinner, W. (2011). Did soil  
751 development limit spruce (*Picea abies*) expansion in the Central Alps during the Holocene?  
752 Testing a palaeobotanical hypothesis with a dynamic landscape model. *Journal of*  
753 *Biogeography*, 38(5), 933-949. <https://doi.org/10.1111/j.1365-2699.2010.02460.x>
- 754 Herren, P. A., Eichler, A., Machguth, H., Papina, T., Tobler, L., Zapf, A., & Schwikowski, M.  
755 (2013). The onset of Neoglaciation 6000 years ago in western Mongolia revealed by an ice  
756 core from the Tsambagarav mountain range. *Quaternary Science Reviews*, 69, 59-68.  
757 <https://doi.org/10.1016/j.quascirev.2013.02.025>
- 758 Hessler, A. E., Brown, P., Byambasuren, O., Cockrell, S., Leland, C., Cook, E., Nachin, B.,  
759 Pederson, N., Saladyga, T., & Suran, B. (2016). Fire and climate in Mongolia (1532–2010  
760 Common Era). *Geophysical Research Letters*, 43(12), 6519-6527.  
761 <https://doi.org/10.1002/2016GL069059>
- 762 Hijjoka, Y., E. Lin, J.J. Pereira, R.T. Corlett, X. Cui, G.E. Insarov, R.D. et al. (2014). Asia. In:  
763 Climate Change 2014: Impacts, Adaptation, and Vulnerability. Part B: Regional Aspects.  
764 Contribution of Working Group II to the Fifth Assessment Report of the Intergovernmental  
765 Panel on Climate Change [Barros, V.R., C.B. Field, D.J. Dokken, M.D. Mastrandrea, K.J.  
766 Mach, T.E. Bilir, M. et al. (eds.)]. United Kingdom and New York, NY: Cambridge  
767 University Press, Cambridge.
- 768 Huang, T. C. (1972). Pollen flora of Taiwan. Taipei: National Taiwan University, Botany Dept.  
769 Press.
- 770 Hurlbert, S. H. (1971). The nonconcept of species diversity: a critique and alternative  
771 parameters. *Ecology*, 52(4), 577-586. <https://doi.org/10.2307/1934145>
- 772 IPCC (2014). Climate Change 2014: Synthesis Report. Contribution of Working Groups I, II  
773 and III to the Fifth Assessment Report of the Intergovernmental Panel on Climate Change  
774 [Core Writing Team, R.K. Pachauri and L.A. Meyer (eds.)]. IPCC, Geneva, Switzerland,  
775 151 pp.
- 776 Khansaritoreh, E., Dulamsuren, C., Klinge, M., Ariunbaatar, T., BatEnerel, B., Batsaikhan, G.,  
777 Ganbaatar, K., Saindovdon, D., Yeruult, Y., Tsogtbaatar, J., Tuya, D., Leuschner, C., &  
778 Markus Hauck, M. (2017). Higher climate warming sensitivity of Siberian larch in small than  
779 large forest islands in the fragmented Mongolian forest steppe. *Global change biology*, 23,  
780 3675–3689. <https://doi.org/10.1111/gcb.13750>
- 781 Klinge, M., Böhner, J., & Lehmkuhl, F. (2003). Climate Pattern, Snow-and Timberlines in the  
782 Altai Mountains, Central Asia (Klimaverhältnisse, Schnee-und Waldgrenzen im Altai  
783 Gebirge, Zentralasien). Bonn: Erdkunde.
- 784 Kuuluvainen, T., Aakala, T., & Várkonyi, G. (2017). Dead standing pine trees in a boreal forest  
785 landscape in the Kalevala National Park, northern Fennoscandia: amount, population

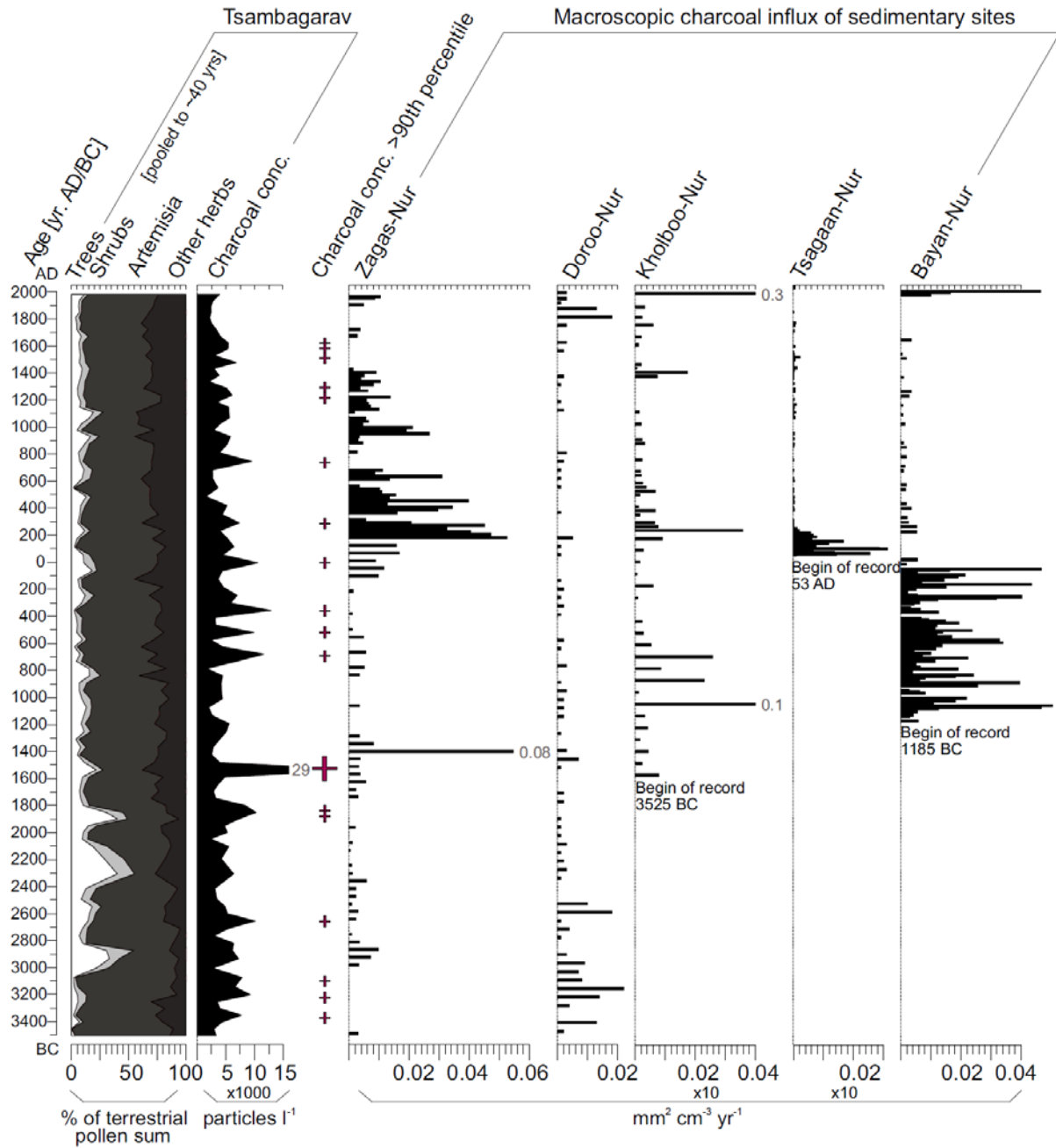
- 786 characteristics and spatial pattern. *Forest Ecosystems*, 4(1), 12.  
787 <https://doi.org/10.1186/s40663-017-0098-7>
- 788 Lang, G. (1994). *Quartäre Vegetationsgeschichte Europas: Methoden und Ergebnisse*. Jena,  
789 Stuttgart, New York: Gustav Fischer.
- 790 Legrand, M., McConnell, J., Fischer, H., Wolff, E. W., Preunkert, S., Arienzo, M., Chellman,  
791 N., Leuenberger, D., Maselli, O., Place, P., Sigl, M., Schüpbach, S., & Flannigan, M. (2016).  
792 Boreal fire records in Northern Hemisphere ice cores: a review. *Climate of the Past*, 12(10),  
793 2033-2059. <https://doi.org/10.5194/cp-12-2033-2016>
- 794 Lehner, F., Coats, S., Stocker, T. F., Pendergrass, A. G., Sanderson, B. M., Raible, C. C., &  
795 Smerdon, J. E. (2017). Projected drought risk in 1.5° C and 2° C warmer climates.  
796 *Geophysical Research Letters*, 44(14), 7419-7428. <https://doi.org/10.1002/2017GL074117>
- 797 Lkhagvadorj, D., Hauck, M., Dulamsuren, C., & Tsogtbaatar, J. (2013). Pastoral nomadism in  
798 the forest-steppe of the Mongolian Altai under a changing economy and a warming climate.  
799 *Journal of arid environments*, 88, 82-89. <https://doi.org/10.1016/j.jaridenv.2012.07.019>
- 800 Liu, H., Cui, H., Pott, R., & Speier, M. (1999). The surface pollen of the woodland–steppe  
801 ecotone in southeastern Inner Mongolia, China. *Review of Palaeobotany and Palynology*,  
802 105(3), 237-250. [https://doi.org/10.1016/S0034-6667\(98\)00074-8](https://doi.org/10.1016/S0034-6667(98)00074-8)
- 803 Liu, H., Park Williams, A., Allen, C. D., Guo, D., Wu, X., Anenkhonov, O. A., Liang, E.,  
804 Sandanov, D. V., Yin, Y., Qi, Z., B & Badmaeva, N. K. (2013). Rapid warming accelerates  
805 tree growth decline in semi-arid forests of Inner Asia. *Global change biology*, 19(8), 2500-  
806 2510. <https://doi.org/10.1111/gcb.12217>
- 807 McDowell, N. G., & Allen, C. D. (2015). Darcy's law predicts widespread forest mortality  
808 under climate warming. *Nature Climate Change*, 5(7), 669.  
809 <https://doi.org/10.1038/nclimate2641>
- 810 MacDonald, G. M., Larsen, C. P., Szeicz, J. M., & Moser, K. A. (1991). The reconstruction of  
811 boreal forest fire history from lake sediments: a comparison of charcoal, pollen,  
812 sedimentological, and geochemical indices. *Quaternary Science Reviews*, 10(1), 53-71.  
813 [https://doi.org/10.1016/0277-3791\(91\)90030-X](https://doi.org/10.1016/0277-3791(91)90030-X)
- 814 Moore, P. D., Webb, J. A., & Collison, M. E. (1991). *Pollen analysis* (2nd ed.). Blackwell  
815 scientific publications.
- 816 Naumov, I. V. (2006). *The history of Siberia*. London, New York: Routledge.
- 817 NOAA (2013). *Ulgii Climate Normals 1961-1990*. National Oceanic and Atmospheric  
818 Administration. Last updated 2013, accessed July 04, 2018.
- 819 Ponomarev, E. I., & Kharuk, V. I. (2016). Wildfire occurrence in forests of the Altai–Sayan  
820 region under current climate changes. *Contemporary Problems of Ecology*, 9(1), 29-36.  
821 <https://doi.org/10.1134/S199542551601011X>
- 822 Rey, F., Gobet, E., Szidat, S., Lotter, A. F., Gilli, A., Hafner, A., & Tinner, W., (2018).  
823 Radiocarbon wiggle matching on laminated sediments delivers high-precision chronologies.  
824 *Radiocarbon*, 1-21. <https://doi.org/10.1017/RDC.2018.47>
- 825 Rogers, J. D. (2012). Inner Asian States and Empires: theories and synthesis. *Journal of*  
826 *Archaeological Research*, 20(3), 205-256. <https://doi.org/10.1007/s10814-011-9053-2>



- 827 Rose, N. L. (2015). Spheroidal carbonaceous fly ash particles provide a globally synchronous  
828 stratigraphic marker for the Anthropocene. *Environmental science & technology*, 49(7),  
829 4155-4162. <https://doi.org/10.1021/acs.est.5b00543>
- 830 Roth, R., & Joos, F. (2013). A reconstruction of radiocarbon production and total solar  
831 irradiance from the Holocene <sup>14</sup>C and CO<sub>2</sub> records: implications of data and model  
832 uncertainties. *Climate of the Past*, 9(4), 1879. <https://doi.org/10.5194/cp-9-1879-2013>
- 833 Rudaya, N. A., Tarasov, P. E., Dorofeyuk, N. I., Kalugin, I. A., Andreev, A. A., Diekmann, B.,  
834 & Daryin, A. V. (2008). Environmental changes in the Mongolian Altai during the Holocene.  
835 *Archaeology, Ethnology and Anthropology of Eurasia*, 36(4), 2-14.  
836 <https://doi.org/10.1016/j.aeae.2009.03.001>
- 837 Rudaya, N., Tarasov, P., Dorofeyuk, N., Solovieva, N., Kalugin, I., Andreev, A., Daryin, A.,  
838 Diekmann, B., Riedel, F., Tserendash, N., & Wagner, M. (2009). Holocene environments  
839 and climate in the Mongolian Altai reconstructed from the Hoton-Nur pollen and diatom  
840 records: a step towards better understanding climate dynamics in Central Asia. *Quaternary*  
841 *Science Reviews*, 28(5), 540-554. <https://doi.org/10.1016/j.quascirev.2008.10.013>
- 842 Sato, T., Kimura, F., & Kitoh, A. (2007). Projection of global warming onto regional  
843 precipitation over Mongolia using a regional climate model. *Journal of Hydrology*, 333(1),  
844 144-154. <https://doi.org/10.1016/j.jhydrol.2006.07.023>
- 845 Schlütz, F., Dulamsuren, C., Wieckowska, M., Mühlenberg, M., & Hauck, M. (2008). Late  
846 Holocene vegetation history suggests natural origin of steppes in the northern Mongolian  
847 mountain taiga. *Palaeogeography, Palaeoclimatology, Palaeoecology*, 261(3), 203-217.  
848 <https://doi.org/10.1016/j.palaeo.2007.12.012>
- 849 Staubwasser, M., & Weiss, H. (2006). Holocene climate and cultural evolution in late  
850 prehistoric–early historic West Asia. *Quaternary Research*, 66(3), 372-387.  
851 <https://doi.org/10.1016/j.yqres.2006.09.001>
- 852 Steinhilber, F., Beer, J., & Fröhlich, C. (2009). Total solar irradiance during the Holocene.  
853 *Geophysical Research Letters*, 36(19). <https://doi.org/10.1029/2009GL040142>
- 854 Stockmarr, J. (1971). Tablets with spores used in absolute pollen analysis. *Pollen et spores*.
- 855 Stritch, L., Shaw, K., Roy, S. & Wilson, B. (2014). *Betula pendula*. The IUCN Red List of  
856 Threatened Species 2014. <http://dx.doi.org/10.2305/IUCN.UK.2014-3.RLTS.T62535A3115662.en>.
- 858 Sun, A., Feng, Z., Ran, M., & Zhang, C. (2013). Pollen-recorded bioclimatic variations of the  
859 last ~ 22,600 years retrieved from Achit Nuur core in the western Mongolian Plateau.  
860 *Quaternary international*, 311, 36-43. <https://doi.org/10.1016/j.quaint.2013.07.002>
- 861 Tarasov, P., Dorofeyuk, N., & Tseva, E. M. (2000). Holocene vegetation and climate changes  
862 in Hoton-Nur basin, northwest Mongolia. *Boreas*, 29(2), 117-126.  
863 <https://doi.org/10.1111/j.1502-3885.2000.tb01205.x>
- 864 Tchebakova, N. M., Blyakharchuk, T. A., & Parfenova, E. I. (2009). Reconstruction and  
865 prediction of climate and vegetation change in the Holocene in the Altai–Sayan mountains,  
866 Central Asia. *Environmental Research Letters*, 4(4), 045025. <https://doi.org/10.1088/1748-9326/4/4/045025>
- 867

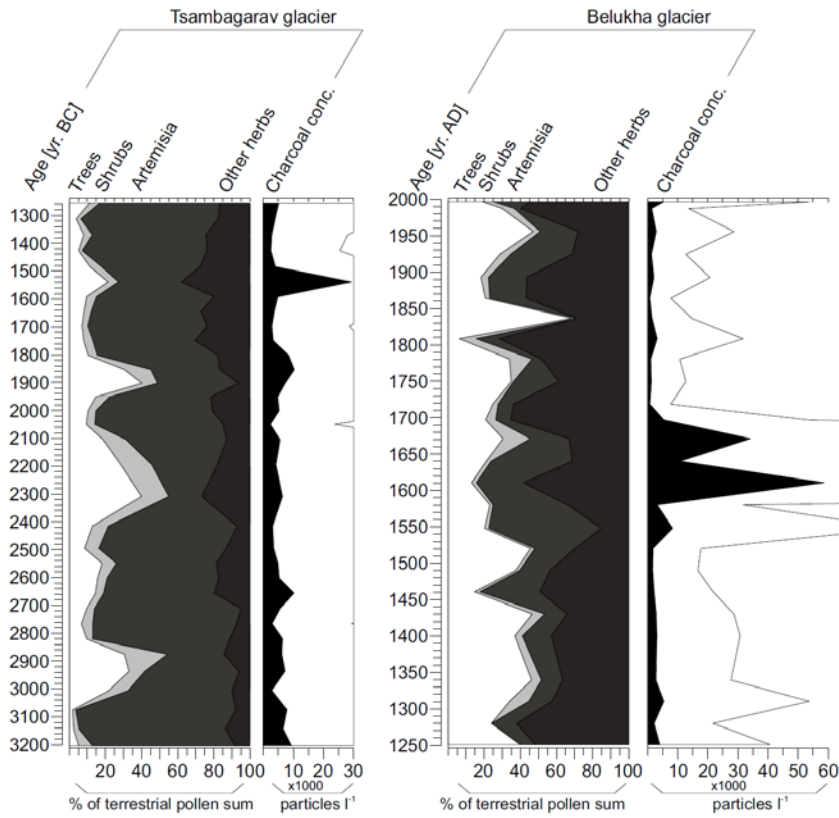
- 868 Ter Braak, C. J., & Prentice, I. C. (1988). A theory of gradient analysis. *Advances in ecological*  
869 *research*, 18, 271-317. [https://doi.org/10.1016/S0065-2504\(03\)34003-6](https://doi.org/10.1016/S0065-2504(03)34003-6)
- 870 Tian, F., Herzsuh, U., Dallmeyer, A., Xu, Q., Mischke, S., & Biskaborn, B. K. (2013).  
871 Environmental variability in the monsoon–westerlies transition zone during the last 1200  
872 years: lake sediment analyses from central Mongolia and supra–regional synthesis.  
873 *Quaternary Science Reviews*, 73, 31-47. <https://doi.org/10.1016/j.quascirev.2013.05.005>
- 874 Tian, F., Herzsuh, U., Mischke, S., & Schlütz, F. (2014). What drives the recent intensified  
875 vegetation degradation in Mongolia–Climate change or human activity?. *The Holocene*,  
876 24(10), 1206-1215. <https://doi.org/10.1177/0959683614540958>
- 877 Tinner, W., Conedera, M., Ammann, B., Gaggeler, H. W., Gedye, S., Jones, R., & Sagesser, B.  
878 (1998). Pollen and charcoal in lake sediments compared with historically documented forest  
879 fires in southern Switzerland since AD 1920. *The Holocene*, 8(1), 31-42.  
880 <https://doi.org/10.1191/095968398667205430>
- 881 Tinner, W., Beer, R., Bigler, C., Clegg, B. F., Jones, R. T., Kaltenrieder, P., van Raden, U. J.,  
882 Gilli, A., & Hu, F. S. (2015). Late-Holocene climate variability and ecosystem responses in  
883 Alaska inferred from high-resolution multiproxy sediment analyses at Grizzly Lake.  
884 *Quaternary Science Reviews*, 126, 41-56. <https://doi.org/10.1016/j.quascirev.2015.08.019>
- 885 Tinner, W., & Hu, F. S. (2003). Size parameters, size-class distribution and area-number  
886 relationship of microscopic charcoal: relevance for fire reconstruction. *The Holocene*, 13(4),  
887 499-505. <https://doi.org/10.1191/0959683603hl615rp>
- 888 TPL (2018). The Plant List, <http://www.theplantlist.org/tpl1.1/record/kew-21520>. Last visited  
889 12.07.2018.
- 890 Tsogtbaatar, J. (2004). Deforestation and reforestation needs in Mongolia. *Forest Ecology and*  
891 *Management*, 201(1), 57-63. <https://doi.org/10.1016/j.foreco.2004.06.011>
- 892 Tsogtbaatar, J. (2013). Deforestation and reforestation of degraded forestland in Mongolia. In:  
893 The Mongolian Ecosystem Network. Japan: Springer.
- 894 Uglietti, C., Zapf, A., Jenk, T. M., Sigl, M., Szidat, S., Salazar Quintero, G. A., & Schwikowski,  
895 M. (2016). Radiocarbon dating of glacier ice: overview, optimisation, validation and  
896 potential. *The Cryosphere*, 10(6), 3091-3105. <https://doi.org/10.5194/tc-10-3091-2016>
- 897 Umbanhowar Jr, C. E., Shinneman, A. L., Tserenkhand, G., Hammon, E. R., Lor, P., & Nail,  
898 K. (2009). Regional fire history based on charcoal analysis of sediments from nine lakes in  
899 western Mongolia. *The Holocene*, 19(4), 611-624.  
900 <https://doi.org/10.1177/0959683609104039>
- 901 Unkelbach, J., Dulamsuren, C., Punsalpaamuu, G., Saindovdon, D., & Behling, H. (2018). Late  
902 Holocene vegetation, climate, human and fire history of the forest-steppe-ecosystem inferred  
903 from core G2-A in the ‘Altai Tavan Bogd’ conservation area in Mongolia. *Vegetation history*  
904 *and Archaeobotany*. <https://doi.org/10.1007/s00334-017-0664-5>
- 905 Volkov, V. V. (1995). Early nomads of Mongolia. In: Davis-Kimball, J., Bashilov, V. A., &  
906 Yablonsky, L. T. (Eds.). *Nomads of the Eurasian steppes in the early Iron Age*. Berkeley:  
907 Zinat.
- 908 Walter, H. (1974). Die Vegetation Osteuropas, Nord-und Zentralasiens. *Vegetations-*  
909 *Monographien der Einzelnen Grossräume, Bd 7*. Stuttgart: Gustav Fischer.

- 910 Wang, W., & Feng, Z. (2013). Holocene moisture evolution across the Mongolian Plateau and  
911 its surrounding areas: A synthesis of climatic records. *Earth-Science Reviews*, 122, 38-57.  
912 <https://doi.org/10.1016/j.earscirev.2013.03.005>
- 913 Wang, Y., Cheng, H., Edwards, R. L., He, Y., Kong, X., An, Z., Wu, J., Kelly, M. J., Dykoski,  
914 C. A., & Li, X. (2005). The Holocene Asian monsoon: links to solar changes and North  
915 Atlantic climate. *Science*, 308(5723), 854-857. <https://doi.org/10.1126/science.1106296>
- 916 Wu, Z. Y. & Raven P. H. (1999). *Flora of China*. Vol. 4 (Cycadaceae through Fagaceae).  
917 Beijing and St. Louis: Science Press and Missouri Botanical Garden Press.
- 918 Van Zeist, W., Woldring, H., & Stapert, D. (2016). Late Quaternary vegetation and climate of  
919 southwestern Turkey. *Palaeohistoria*, 17, 53-143.
- 920 Xu, C., Liu, H., Anenkhonov, O. A., Korolyuk, A. Y., Sandanov, D. V., Balsanova, L. D.,  
921 Naidanov, B. B., & Wu, X. (2017). Long-term forest resilience to climate change indicated  
922 by mortality, regeneration, and growth in semiarid southern Siberia. *Global change biology*,  
923 23(6), 2370-2382.
- 924 Zhao P, Xu C, Zhou M, Zhang B, Ge P, Zeng N, & Liu H. (2018) Rapid regeneration offsets  
925 losses from warming-induced tree mortality in an aspen-dominated broad-leaved forest in  
926 northern China. *PLoS ONE* 13(4), e0195630. <https://doi.org/10.1371/journal.pone.0195630>



928  
929  
930  
931

**Figure A1** Comparison of Tsambagarav vegetation and fire reconstruction (charcoal concentrations and charcoal concentrations exceeding 90-percentile of all samples) with local fire reconstructions (macroscopic charcoal influx of particles >180µm) from lakes in western Mongolia (Umbanhowar et al., 2009) over the past 5500 years.



932  
 933  
 934  
 935  
 936

**Figure A2** Comparison of forest phases recorded in glacier archives in the Mongolian and Russian Altai. Left: Tsambagarav main pollen diagram (percentages) and charcoal concentrations (particles l<sup>-1</sup>) during maximum afforestation (3000–1800 BC), right: Belukha main pollen diagram and charcoal concentrations 1250–1990 AD (Eichler et al., 2011). Hollow curves = 10x exaggeration.